Cryptic diversity in the whip spider genus *Paraphrynus* (Amblypygi: Phrynidae): integrating morphology, karyotype and DNA

MICHAEL SEITER *,[1], AZUCENA C. REYES LERMA[2], JIŘÍ KRÁL[2], ALEXANDR SEMBER[2], KLÁRA DIVIŠOVÁ[2], JOSÉ G. PALACIOS VARGAS[3], PÍO A. COLMENARES[4], STEPHANIE F. LORIA[4] & LORENZO PRENDINI[4]

[1] Department of Evolutionary Biology, Unit Integrative Zoology, University of Vienna, Althanstraße 14, 1090 Vienna, Austria; Michael Seiter [michael.seiter@univie.ac.at] — [2] Laboratory of Arachnid Cytogenetics, Department of Genetics and Microbiology, Faculty of Science, Charles University, Viničná 5, 128 44 Prague 2, Czech Republic; Azucena C. Reyes Lerma [areyes.lerma@gmail.com]; Jiří Král [spider@natur. cuni.cz]; Alexandr Sember [alexandr.sember@seznam.cz]; Klára Divišová [Dweep2@seznam.cz] — [3] Ecología y Sistemática de Microartrópodos, Departamento de Ecología y Recursos Naturales, Facultad de Ciencias, Universidad Nacional Autónoma de México, Av. Universidad 3000, 04510 México City, Mexico; José G. Palacios Vargas [troglolaphysa@hotmail.com] — [4] Arachnology Lab, Division of Invertebrate Zoology, American Museum of Natural History, Central Park West at 79th Street, New York, NY 10024-5192, USA; Pío A. Colmenares [pcolmenares@amnh.org]; Stephanie F. Loria [sloria@amnh.org]; Lorenzo Prendini [lorenzo@amnh.org] — * Corresponding author

Abstract. The whip spider (Amblypygi) genus *Paraphrynus* Moreno, 1940 is distributed from the southern U.S.A. to the Greater Antilles and northern South America. Mexico is the diversity hotspot of the genus where many morphologically similar species occur, often in close geographical proximity. The present contribution aimed to resolve the diversity and phylogenetic relationships within the *aztecus* group of species, which includes the type species, *Paraphrynus mexicanus* (Bilimek, 1867), resulting in the description of a new species from Mexico, *Paraphrynus pseudomexicanus* sp.n. This is the first study to integrate morphology, karyotype, and DNA for species delimitation in whip spiders. Karyotype data have not been previously used for the taxonomy of these arachnids. Sequence analysis included seven species of the *aztecus* group, two other species of *Paraphrynus*, and an outgroup species of the putative sister genus, *Phrynus* Lamarck, 1801. Two nuclear genes (18S rDNA and 28S rDNA) and three mitochondrial genes (12S rDNA, 16S rDNA, and Cytochrome *c* Oxidase Subunit I) were analyzed phylogenetically. Hypotheses of karyotype evolution of *Paraphrynus* are consistent with conclusions based on the morphological and molecular data. The ancestral karyotype of the *aztecus* group probably consisted of a relatively low number of biarmed chromosomes. Diploid numbers decreased by cycles consisting of inversion and consequent centric fusion during the evolution of the clade comprising *P. mexicanus* and *P. pseudomexicanus*.

Key words. Arachnida, centric fusion, chromosome, evolution, inversion, molecular systematics, phylogeny, new species, taxonomy.

1. Introduction

Whip spiders (Amblypygi), an ancient order of arachnids, dating back to the Carboniferous (DUNLOP 1994), and comprising approximately 220 extant species in 18 genera and five families (MIRANDA et al. 2018), occur mainly in tropical and subtropical regions (WEYGOLDT 2000). Although whip spiders have been relatively neglected, compared to more diverse arachnid orders, more attention has been paid to their morphology, systematics and biology in recent years (e.g. CHAPIN 2014a,b; CHAPIN & REED-GUY 2017; HEBETS et al. 2014a,b; SEITER et al. 2017; WOLFF et al. 2016, 2017; FILIPPOV et al. 2017). Many new species were described in the past decade, and yet the systematics of whip spiders has to some extent been constrained by their conservative morphology. Only

one study to date explored other sources of evidence, in addition to morphology, for resolving species limits among whip spiders using three different sources of evidence, namely behaviour, morphology and DNA (Prendini et al. 2005).

One source of taxonomic difficulty, among several in the order, is the Neotropical genus *Paraphrynus* Moreno, 1940, a group of medium-sized to large whip spiders in the family Phrynidae Thorell, 1883, distributed from the southwestern U.S.A., through Central America and the Greater Antilles, to northern South America (Harvey 2003). These whip spiders inhabit caves, rock walls, and the trunks of large trees, in tropical and subtropical forests. *Paraphrynus* is most diverse in Mexico, where 15 of its 20 species occur (Armas 2012; Armas & Trujillo 2018).

Mullinex (1975) divided the species of *Paraphrynus* into the *aztecus*, *laevifrons*, and *raptator* groups. The study presented here addresses the *aztecus* group, which was demonstrated to be monophyletic in a phylogenetic analysis based on morphological characters conducted in the framework of a M.S. thesis (Ballesteros 2010). As originally defined by Mullinex (1975), the *aztecus* group comprised five species, i.e., *P. aztecus* (Pocock, 1894), *P. velmae* Mullinex, 1975, *P. baeops* (Mullinex, 1975), *P. mexicanus* (Bilimek, 1867) and *P. pococki* Mullinex, 1975. However, Mullinex (1975) also recognized three different forms of *P. mexicanus*, i.e., the Cacahuamilpa form (type locality in Mexico), the Arizona form, and the Cuban form. Quintero (1983) subsequently described as *Paraphrynus cubensis* Quintero, 1983 and removed *P. velmae* from the *aztecus* group. More recently, Armas (2012) described the Arizona form as *P. carolynae* Armas, 2012. Consequently, the *aztecus* group presently contains six species, i.e., *P. aztecus*, *P. mexicanus*, *P. carolynae*, *P. cubensis*, *P. baeops* and *P. pococki*. The group is diagnosed on the basis of the following combination of characters: pedipalp basitarsus dorsal spine 1 longer than spine 3; no minute spine on pedipalp basitarsus proximal to dorsal spine 1; pedipalp tibia dorsal spine 7 (if present) shorter than spine 2; pedipalp femur ventral spine III almost as long as spine I and spine II (reduction in length). Additionally, all species of the *aztecus* group, except for *P. aztecus*, have reduced median ocular tubercles and median ocelli, and only a single tooth on the retrolateral margin of the proximal cheliceral segment. *Paraphrynus aztecus* exhibits fully developed median ocelli and two cheliceral teeth on the retrolateral margin of the proximal cheliceral segment (Ballesteros 2010; Mullinex 1975; Quintero 1983; Armas 2012).

The present study aimed to resolve the diversity and phylogenetic relationships within the *aztecus* group, by integrating data from morphology, karyotype, and DNA sequences. A new species of *Paraphrynus* is described from Mexico and its morphology compared with the closely related species, *P. carolynae* and *P. mexicanus*. A phylogenetic analysis based on DNA sequences is presented for all species of the *aztecus* group and relevant outgroups. Finally, the karyotype of one species of *Phry-*

nus, i.e. *P. marginemaculatus* C.L. Koch, 1841, and five species of *Paraphrynus*, i.e., *P. aztecus*, *P. carolynae*, *P. cubensis*, *P. mexicanus*, and *P. robustus*, is presented, permitting a hypothesis of karyotype evolution in *Paraphrynus*, consistent with conclusions based on the morphological and molecular data, to be presented.

Karyotype data could be an effective tool to differentiate closely related species within morphologically conservative orders like Amblypygi. Considerable intrageneric differentiation of karyotypes, sufficient for use in cytotaxonomy and phylogenetic reconstructions, has been reported in most other arachnid orders analyzed chromosomally so far, namely acariform and parasitiform mites (Norton et al. 1993), harvestmen (Tsurusaki et al. 2020), palpigrades (Král et al. 2008), pseudoscorpions (Šťáhlavský et al. 2020), scorpions (Schneider et al. 2020), and some groups of spiders (Araujo et al. 2020). Karyotypes of whip spiders also exhibit a high level of intrageneric differentiation (J. Král, unpublished data). The present study is the first to make use of the karyotype, in combination with other sources of evidence, for species delimitation in whip spiders (Paula-Neto et al. 2013). These data illustrate the importance of an integrative approach (Dayrat 2005) to the systematics of whip spiders.

2. Material and methods

2.1. Taxon sampling and material examined

The new species of *Paraphrynus*, described in the present contribution, was compared with congeners and with the putative sister genus *Phrynus* Lamarck, 1801 as the outgroup. Material used for morphology is deposited in the collection of Naturhistorisches Museum, Wien, Austria (NHMW); for chromosome analysis in the Department of Genetics and Microbiology, Charles University, Prague, Czech Republic (JK); and tissue samples for DNA extraction in the Ambrose Monell Cryocollection at the American Museum of Natural History (AMNH), New York, U.S.A. (Electronic Supplement S1).

The phylogenetic analysis included eleven terminal taxa, representing all six described species of the *aztecus* group, i.e., *P. aztecus*, *P. baeops*, *P. carolynae*, *P. cubensis*, *P. mexicanus* and *P. pococki*, two samples of the new species, two other species of *Paraphrynus*, i.e., *P. robustus* (Franganillo, 1931) and *P. viridiceps* (Pocock, 1894), and *Phrynus marginemaculatus* as an outgroup species.

2.2. Morphology

Material was examined with a Nikon SMZ25 stereomicroscope equipped with a DS-Ri2 microscope camera (software NIS-Elements BR). Digital images were pro-

Table 1. Primers used for amplification of 12S rDNA (12S), 16S rDNA (16S), 18S rDNA (18S), 28S rDNA (28S), and gene of Cytochrome *c* Oxidase subunit I (COI) in phylogenetic analysis of *Paraphrynus* Moreno, 1940 whip spiders.

Gene	Primer	Alias	Sequence	Citation
12S	12Sai	SR-N-14588	A A A C T A G G A T T A G A T A C C C T A T T A T	Kocher et al. (1989)
	12Sbi	SR-J-14233	A A G A G C G A C G G G C G A T G T G T	Kocher et al. (1989)
16S	16Sar	LR-N-13398	C G C C T G T T T A T C A A A A A C A T	Simon et al. (1994)
	16Sbr	LR-J-12887	C T C C G G T T T G A A C T C A G A T C A	Simon et al. (1994)
18S	18S1F		T A C C T G G T T G A T C C T G C C A G T A G	Wheeler et al. (1993)
	18S5R		C T T G G C A A A T G C T T T C G C	Wheeler et al. (1993)
	18S3F		G T T C G A T T C C G G A G A G G G A	Wheeler et al. (1993)
	18Sbi		G A G T C T C G T T C G T T A T C G G A	Wheeler et al. (1993)
	18SA2.0		A T G G T T G C A A A G C T G A A A C	Wheeler et al. (1993)
	18S9R		G A T C C T T C C G C A G G T T C A C C T A C	Wheeler et al. (1993)
28S	28Sa	D3A	G A C C C G T C T T G A A G C A C G	Nunn et al. (1996)
	28Sbout		C C C A C A G C G C C A G T T C T G C T T A C C	Prendini et al. (2005)
COI	LCO	LCO-1490-J-1514	G G T C A A C A A A T C A T A A A G A T A T T G G	Folmer et al. (1994)
	HCO		T A A A C T T C A G G G T G A C C A A A A A A T C A	Folmer et al. (1994)

cessed using Adobe Photoshop 8.0. Most diagnostic structures used for species delimitation concern the gonopods and pedipalps. Descriptions of the male reproductive structures follow GIUPPONI & KURY (2013). The nomenclature of pedipalp segments and spines follows QUINTERO (1981), with pedipalp divided into trochanter, femur, tibia, basitarsus, pretarsus and tarsus (claw), pedipalp dorsal spines indicated by Arabic numerals, and ventral spines by Roman numerals, following WEYGOLDT (2000). Pedipalp basitarsal spination differs among conspecifics and is open to interpretation, following SEITER & LANNER (2017) and SEITER & WOLFF (2017). Trichobothrial nomenclature on the distitibia and distal basitibia of leg IV follows WEYGOLDT (2000).

Abbreviations: bta = pedipalp basitarsal spination; co-ls = pretarsus, row of long setae; co-ss = pretarsus, row of short setae; cs = claw-like sclerites; D/V = dorsal/ventral pedipalpal spine counts; dt = distitibia; Fi = fistula; FP = carapace, frontal process; GO = gonopod (♀); LaM = male genitalia, *lamina medialis*; LoD = male genitalia, *lobus dorsalis*; LoL1 = male genitalia, *lobus lateralis primus*; LoL2 = male genitalia, *lobus lateralis secundus*; lsmd-s = basitarsus, large submedial dorsal spine; lsmv-s = basitarsus, large submedial ventral spine; PI = gonopod, *processus internus*; rs = basitarsus, row of setae basal to cleaning organ; sp1 – sp4 = basitarsus, dorsal spines 1 – 4; spI, spII = basitarsus, ventral spines I and II. A specific terminology concerns the trichobothria of leg IV: bc = basocaudal; bf = basofrontal; bt = basitibial; sbf = sub-basofrontal; sc-x = x series caudal; sf-x = series frontal; stc-x = x series subterminal caudal; stf-x = x series subterminal frontal; tc = terminal caudal; tf = terminal frontal; tm = terminal medial.

2.3. DNA sequencing

Genomic DNA was extracted from leg muscle tissue using a Qiagen DNeasy Blood and Tissue extraction kit following manufacturer's protocols. Extracted DNA was amplified for five gene loci, selected based on their ability to provide resolution at various taxonomic levels (PRENDINI et al. 2005), in overlapping fragments using universal eukaryote and arachnid-specific primers (Table 1): three mitochondrial loci, i.e., Cytochrome *c* Oxidase Subunit I (hereafter, COI), 12S rRNA (12S) and 16S rRNA (16S), and two nuclear loci, i.e., 18S rRNA (18S) and 28S rRNA (28S). The polymerase chain reaction was performed in an Epicenter thermocycler (Eppendorf) using GoTaq polymerase (Promega). DNA was verified on a 1.2% agarose gel stained with Sybr safe DNA gel stain (Invitrogen), and subsequently purified using the Ampure DNA purification system (Agencourt) on a Biomek NX robot (Beckman-Coulter). Cycle sequencing was conducted using Big Dye v1.1 and automated Sanger dideoxy sequencing of single-stranded DNA performed on an Applied Biosystems Inc. Prism™ 3730x. Paired-strand reads were aligned using Sequencher™ and edited by hand. Fifty-four DNA sequences were generated (Table 2). The sequences were complete for all individuals, except *P. baeops* (extract AMCC [LP 8667]), which was missing the 16S locus.

2.4. Alignment, phylogenetic analysis and genetic divergence

Multiple sequence alignments for individual gene partitions were performed with the online alignment program, MAFFT (KATOH & KIMA 2002; KATOH et al. 2005), using the G-INS-i and Q-INS-i strategies, recommended by the authors for fewer than 200 sequences with global homology, and PAM1/K=2 matrix parameter, recommended by the authors for aligning sequences of closely related taxa. The L-INS-i alignment strategy was also investigated, using the 'leavegappyregion' option in the desktop version of MAFFT. There was no length variation among the COI and 18S sequences, and minor length variation among the 28S (a single nucleotide), 16S (no more than fourteen nucleotides), and 12S (twenty-four nucleotides) sequences (Table 3). The resulting alignments were man-

Table 2. Terminal taxa, countries and states or provinces of origin, Ambrose Monell Cryocollection (AMCC) tissue catalog numbers, and GenBank accession codes for 12S rDNA (12S), 16S rDNA (16S), 18S rDNA (18S), 28S rDNA (28S) and Cytochrome *c* Oxidase Subunit I (COI) sequences used in phylogenetic analysis of *Paraphrynus* Moreno, 1940 whip spiders.

Species	AMCC	Country, State/Prov.	12S	16S	18S	28S	COI
P. aztecus	2096	Mexico, Veracruz	MT753014	MT734759	MT734769	MT734785	MT738748
P. baeops	8667	Mexico, San Luis Potosí	MT753015	----------	MT734770	MT734786	MT738749
P. carolynae	14444	U.S.A., Arizona	MT753016	MT734760	MT734771	MT734787	MT738750
P. cubensis	13883	Cuba, Artemisa	MT753017	MT734761	MT734772	MT734788	MT738751
P. mexicanus	15431	Mexico, Guerrero	MT753018	MT734762	MT734773	MT734789	MT738752
P. pococki	2091	Mexico, San Luis Potosí	MT753019	MT734763	MT734774	MT734790	MT738753
P. pseudomexicanus	14443	Mexico, Morelos	MT753020	MT734764	MT734775	MT734791	MT738754
P. pseudomexicanus	14450	Mexico, Morelos	MT753021	MT734765	MT734776	MT734792	MT738755
P. robustus	13872	Cuba, Guantánamo	MT753022	MT734766	MT734777	MT734793	MT738756
P. viridiceps	13881	Cuba, Pinar del Río	MT753023	MT734767	MT734778	MT734794	MT738757
Phrynus marginemaculatus	14072	Dom. Rep., Bahoruco Prov.	MT753024	MT734768	MT734779	MT734795	MT738758

Table 3. Aligned length (base-pairs, bp) and model selected with JModelTest v2.1.6 using the Akaike Information Criterion (AIC) for 12S rDNA (12S), 16S rDNA (16S), 18S rDNA (18S), 28S rDNA (28S) and Cytochrome *c* Oxidase Subunit I (COI) gene loci used in phylogenetic analysis of *Paraphrynus* Moreno, 1940 whip spiders.

	Length (bp)			**Model** (AIC)		
Locus	G-INS-i	L-INS-i	Q-INS-i	G-INS-i	L-INS-i	Q-INS-i
12S	392	392	416	HKY+Γ	HKY+Γ	GTR+I+Γ
16S	531	530	544	GTR+I+Γ	GTR+I+Γ	GTR+I+Γ
18S	1760	1760	1760	HKY+I	HKY+I	HKY+I
28S	530	530	531	GTR+I	GTR+I	GTR+I
COI	658	658	658	GTR+I+Γ	GTR+I+Γ	GTR+I+Γ

Table 4. Sensitivity of DNA sequence data for phylogenetic analysis of *Paraphrynus* Moreno, 1940 whip spiders, to alignment method (G-INS-i vs. Q-INS-i) and gap treatment (as missing data or a fifth character state), as reflected by the number and length of most parsimonious trees (MPTs) recovered with equal weighting (EW).

	G-INS-i		**L-INS-i**		**Q-INS-i**	
Alignment Length	3870	3870	3871	3871	3909	3909
Informative Nucleotides	559	516	564	514	538	487
Informative Gaps	missing (?)	43	missing (?)	50	missing (?)	51
Informative Sites	559	559	564	564	538	538
MPTs (EW)	1	1	1	1	2	1
MPT length (EW)	1639	1773	1632	1788	1542	1759

Table 5. Sensitivity of DNA sequence data for phylogenetic analysis of whip spiders in the genus *Paraphrynus* Moreno, 1940, to alignment method (G-INS-I, L-INS-i and Q-INS-i), optimality criterion (Maximum Likelihood, ML, Bayesian Inference, BI, or parsimony), weighting regime (equal weighting, EW vs. implied weighting, IW, with five k values) and gap treatment (as missing data, ?, or a fifth character state, -), as reflected by the recovery of four clades of *Paraphrynus*: **A**: ((*P. aztecus* (*P. mexicanus P. pseudomexicanus*)); **B**: ((*P. cubensis* (*P. mexicanus P. pseudomexicanus*)); **C**: ((*P. aztecus P. cubensis*) (*P. mexicanus P. pseudomexicanus*)); **D**: (*P. aztecus P. cubensis* (*P. mexicanus P. pseudomexicanus*)); **E**: (((*P. baeops* (*P. carolynae P. pococki*)) (*P. aztecus P. cubensis P. mexicanus P. pseudomexicanus*))); **F**: ((*P. carolynae P. pococki*) ((*P. baeops* (*P. aztecus P. cubensis P. mexicanus P. pseudomexicanus*))); **G**: (*P. baeops* (*P. carolynae P. pococki*) (*P. aztecus P. cubensis* (*P. mexicanus P. pseudomexicanus*))) .

Alignment	Gaps	Optimality Criterion	Weighting Regime	A	B	C	D	E	F	G
G-INS-i	gaps (?)	ML		x				x		
		BI					x	x		
		parsimony	EW, IW: *k* = 1, 3, 10, 60, 100	x				x		
	gaps (-)		EW, IW: *k* = 1, 3, 10, 60, 100	x				x		
L-INS-i	gaps (?)	ML			x			x		
		BI					x	x		
		parsimony	EW, IW: *k* = 3, 10, 60, 100		x			x		
			IW: *k* = 1	x				x		
	gaps (-)		EW, IW: *k* = 1, 3, 10, 60, 100	x				x		
Q-INS-i	gaps (?)	ML, BI				x		x		
		parsimony	EW			x				x
			IW: *k* = 1, 3, 10, 60, 100			x		x		
	gaps (-)		EW, IW: *k* = 10, 60, 100			x			x	
			IW: *k* = 1, 3			x		x		

Table 6. Diagnostic characters for three members of the *aztecus* group of *Paraphrynus* Moreno, 1940 whip spiders from North America. Abbreviations: [1]counts in parentheses from Armas (2012), those marked 'x' not mentioned; [2]mean; bta = pedipalp basitarsus spination; CT = cerotegument; D/V = dorsal/ventral spine counts; dt = distitibia; FP = frontal process; GO = gonopod (♀); lh = lateral horns; LaM = *lamina medialis*; PI = gonopod *processus internus*, SP = spermatophore organ (♂).

Character	*P. carolynae*	*P. mexicanus*	*P. pseudomexicanus*
Carapace tubercles	fine	coarse	coarse
Carapace FP (♀)	enlarged	obsolete	obsolete
Tritosternum (base)	densely hirsute	sparsely hirsute	densely hirsute
Chelicera dentition	3+1/4	3+1/5	3+1/5
Chelicera tubercles	obsolete	obsolete	present
Pedipalp femur D/V	6/6	6/6	7/8
Pedipalp tibia D/V	8/7 (6–9/x)[1]	8–9/6 (7/x)[1]	9/6
Pedipalp bta D/V	4/3 (3/3)[1]	4/3 (3/3)[1]	4/3
Pedipalp surface	smooth	rough	rough
Tibial articles I[2]	29	27	27
Tarsal articles I[2]	60	59	59
Trichobothria dt IV	24	21	22
GO sclerotization	partly, centric	evenly	evenly
GO base	slender	broadened	broadened
GO distal	markedly curved	moderately curved	rectilinear
SP organ PI	weakly developed	weakly developed	well-developed
SP organ LaM	well-developed	weakly developed	weakly developed
CT globule surface	wrinkled	unknown	network of pores
CT colloid particles	large crystals	unknown	small crystals

ually checked in Geneious (Biomatters, Ltd). The concatenated G-INS-i alignment was 3870 base-pairs (bp) in length with 559 sites, including 43 gaps, parsimony-informative. The concatenated Q-INS-i alignment was 3909 bp in length with 538 sites, including 51 gaps, parsimony-informative (Table 4). The concatenated L-INS-i alignment was 3871 bp in length with 564 sites including 50 gaps, parsimony-informative (Table 4). The nucleotide composition was 26% A, 21% C, 26% G and 27% T.

The concatenated Q-INS-i, G-INS-i, and L-INS-i alignments, partitioned by gene, were each analyzed with Maximum Likelihood (ML) in RaxML-HPC v8 (STAMATAKIS 2006, 2014). All partitions were analyzed using a GTR+Γ model (YANG 1994). The tree was rooted on *P. marginemaculatus*. A rapid bootstrap analysis with 1000 replicates was used to search for the ML tree (STAMATAKIS 2014). Bayesian Inference (BI) was also performed on the Q-INS-i, G-INS-i, and L-INS-i alignments using MrBayes v3.2.7 (RONQUIST & HUELSENBECK 2003) on the CIPRES gateway (https://www.phylo.org) with the following settings applied to all partitions: mcmc; nchains=4; sample frequency=1000; diagnosing frequency=1000; burnin=0.25; savebrlens=yes. Models for each gene were selected using the Akaike Information Criterion (AIC) after testing 24 substitution models in jModelTest v2.1.6 (GUINDON & GASCUEL 2003; DARRIBA et al. 2012) on the CIPRES gateway (Table 4). Analyses with BI were terminated after 25 million generations when the standard deviation of the split frequencies was below 0.01.

A sensitivity analysis was conducted to assess the sensitivity of the data to different parameters (alignment method, weighting regime and gap treatment), following PRENDINI (2000). Both concatenated alignments were analyzed with parsimony under equal weighting and implied weighting (GOLOBOFF 1993), with five values for the concavity constant ($k = 1, 3, 10, 60, 100$) and gaps treated as missing data or as a fifth character state. Parsimony analyses were conducted in TNT v1.1 (GOLOBOFF et al. 2003, 2008) with uninformative characters inactivated, using a script by SANTIBÁÑEZ et al. (2014), which includes tree drifting, mixed sectorial search and tree fusing for the tree search: hold 10000; rseed1; xm: noverb nokeep; rat: it 0 up 4 down 4 au 0 num 36 give 99 equa; dri: it 10 fit 1.00 rfi 0.20 aut 0 num 36 give 99 xfa 3.00 equa; sec: mins 45 maxs 45 self 43 incr 75 minf 10 god 75 drift 6 glob 5 dglob 10 rou 3 xss 10−14+2 noxev noeq; tf: rou 5 minf 3 best ke nochoo swap; xm: level 10 nochk rep 50 fuse 3 dri 10 rss css noxss mult nodump conse 5 conf 75 nogive notarg upda autoc 3 xmix; xm; xmult (Table 5).

Uncorrected pairwise genetic distances of the COI locus were calculated in Mega v10.1.7 (KAMURA et al. 2018; STECHER et al. 2020) for eight *Paraphrynus* terminals representing all six described species in the *P. aztecus* group and two samples of the new species, *P. pseudomexicanus*.

2.5. Karyotype

Karyotype data were obtained for *Phrynus marginemaculatus* and six species of *Paraphrynus* (Electronic Supplement S1). Chromosomes were prepared from the gonads of nymphs or adults. Numerous mitoses and complete sequence of meiosis were found in the testes of adult males. Chromosomes were prepared with a spreading technique (DOLEJŠ et al. 2011). Preparations were stained with 5% Giemsa solution in Sörensen buffer (pH 6.8) for 30 min
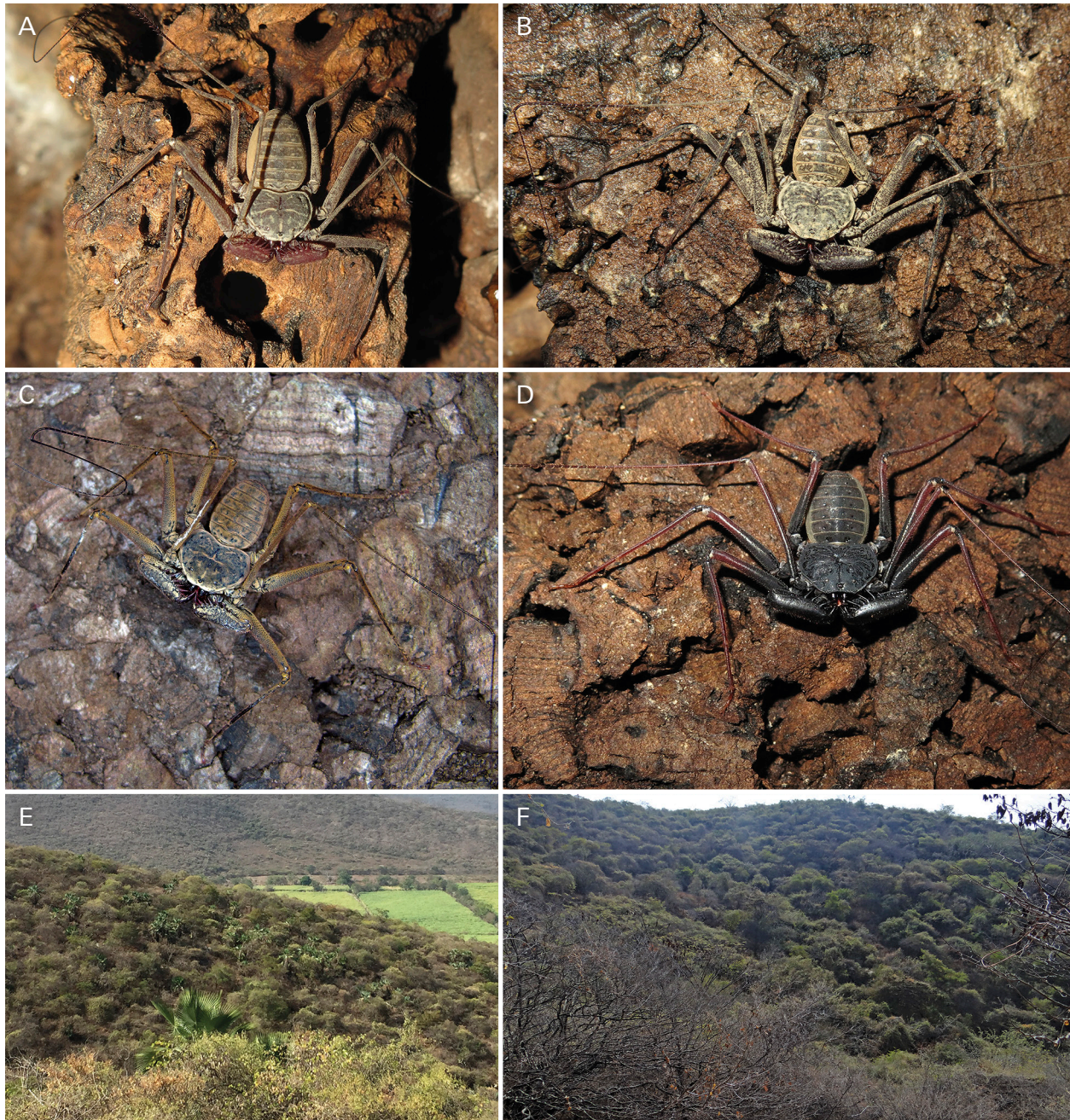
Fig. 1. *Paraphrynus* Moreno, 1940, habitus in life and type locality of the new species. **A**, **B**, **E**, **F**: *Paraphrynus pseudomexicanus* sp.n., female, habitus (**A**, **B**) and type locality, Cerro de los Túneles, Morelos, Mexico (**E**, **F**). **C**: *Paraphrynus mexicanus* (Bilimek, 1867), male, Juxtlahuaca Cave, Guerrero, Mexico. **D**: *Paraphrynus carolynae* Armas, 2012, male, Tucson, Arizona, U.S.A.

and observed under a BX 50 microscope (Olympus). Images were obtained with a DP 71 CCD camera (Olympus) using an oil immersion lens (100×).

At least two plates of metaphase II (formed by two sister metaphases II) per species were used to evaluate the morphology of chromosomes and construct the karyotypes. Relative chromosome lengths were calculated as a percentage of the total chromosome length of the diploid set. Chromosome morphology was classified based on position of the centromere according to LEVAN et al. (1964). Chromosome measurements were taken using IMAGE J software. Karyotypes were constructed using the software Corel PHOTO-PAINT X4.

3. Results

3.1. Morphology

Morphology suggested a close relationship between *P. carolynae*, *P. mexicanus*, and the new species, based on the following characters. The count of dorsal and ventral spines on the pedipalp basitarsus (four dorsal and three ventral) is identical in all three species. The number of tibial and tarsal articles of leg I, as well as the form and shape of the frontal process, are identical in *P. mexicanus* and the new species. The spermatophore organs are gen-
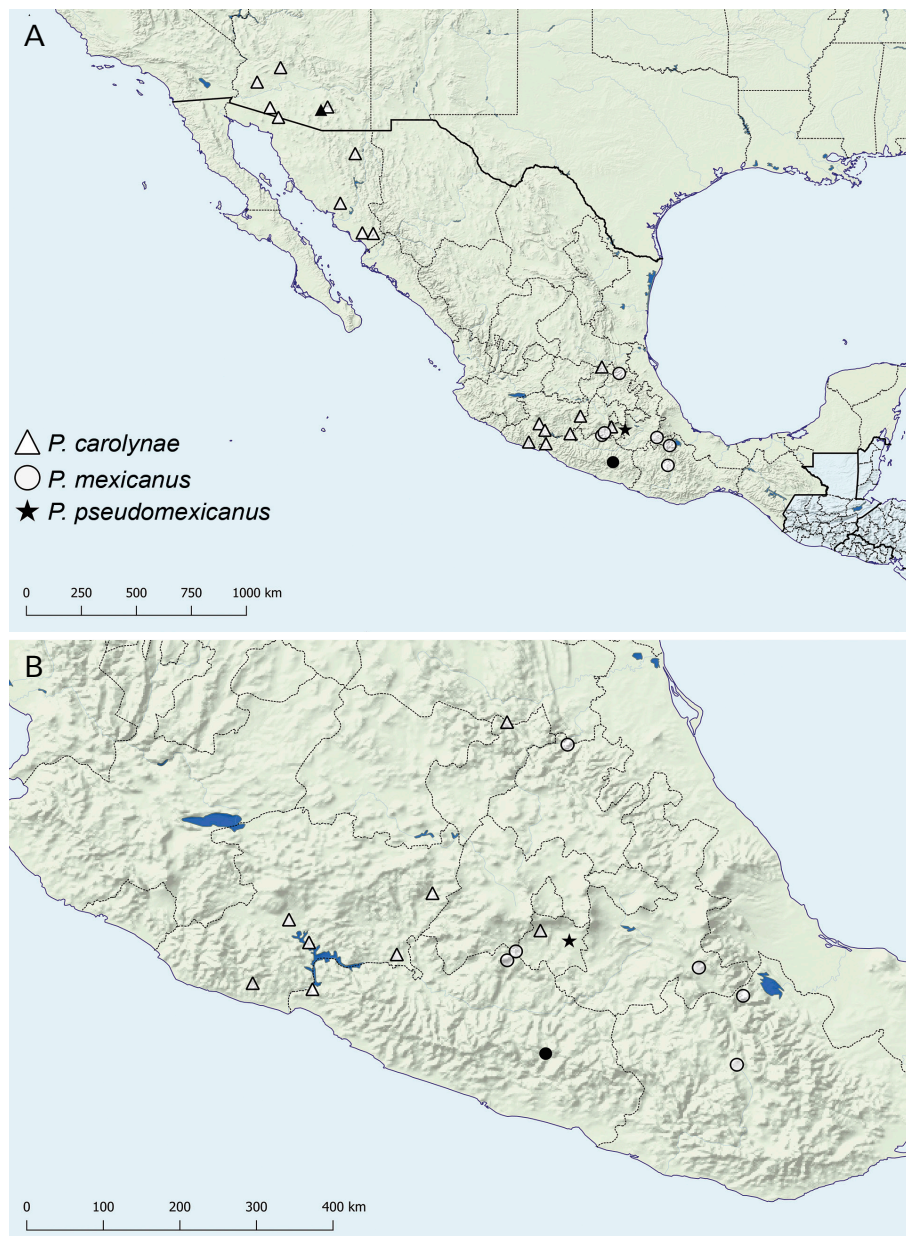
Fig. 2. Maps of southern part of North America (**A**) and southern part of central Mexico (**B**), plotting known distributions of *Paraphrynus pseudomexicanus* sp.n. (black star), *Paraphrynus mexicanus* (Bilimek, 1867) (circles), and *Paraphrynus carolynae* Armas, 2012 (triangles) compiled from records in Armas (2012), Armas & Cuéllar-Balleza (2018), Harvey (2003), and the present study. Black symbols indicate localities from which specimens were used for morphology, DNA extraction and cytogenetics.

erally similar in all three species (Fig. 11). Although the gonopod *processus internus* is well developed in *P. pseudomexicanus* and weakly developed in *P. carolynae* and *P. mexicanus*, the *lamina medialis* is well developed in *P. carolynae* and weakly developed in the other two species. In contrast to the male spermatophore, the female reproductive organs are very distinct among the three species (Fig. 11). Whereas the gonopods of *P. mexicanus* and *P. pseudomexicanus* exhibit a broadened base, the distal parts of the sclerotized hooks are curved in the former and rectilinear in the latter. The gonopods of *P. carolynae* exhibit a slender base, and are predominantly narrow, with a marked curvature distally.

Despite the similarity among the three species, several diagnostic characters were identified to support the new species, i.e., the presence of cheliceral tubercles; the spination pattern of the pedipalp femur (7 and 8 major spines on the dorsal and ventral margin, respectively)

(Figs. 5, 6); the number of tibial (27) and tarsal (59) articles of leg I (Table 6); and the number of trichobothria on the distitibia of leg IV (22) (Fig. 9, Table 6).

3.2. Description of new species

Genus *Paraphrynus* Moreno, 1940

Paraphrynus pseudomexicanus sp.n.

Material examined. *Type material.* Holotype: 1 ♀ (NHMW 27612), MEXICO: *Morelos*: Ayala Municipality: Anenecuilco surrounding, Cerro de los Túneles, 18°47′19″N 99°01′34″W, xi.2010, J. Král. Paratypes: 1 ♂ (NHMW 27613), 2 ♂♂, 2 ♀♀ (NHMW 27614), same data as holotype; 3 ♂♂, 3 ♀♀ (NHMW 29177), same data as holotype, except "captive bred, 17.vi.2013"; 1 ♂ [leg] (AMCC [LP 14450]), 13.ix.2012, J. Král, 1 ♂ (karyotype, JK), same data as holotype, except "captive bred, 17.vi.2013, M. Seiter."

Fig. 3. *Paraphrynus* Moreno, 1940, carapace, anterodorsal aspect (**A**, **C**, **E**), and pedipalp coxae and anterior part of tritosternum, ventral aspect (**B**, **D**, **F**). **A**, **B**: *Paraphrynus pseudomexicanus* sp.n., holotype female (NHMW 27612), Cerro de los Túneles, Morelos, Mexico. **C**, **D**: *Paraphrynus mexicanus* (Bilimek, 1867), female (NHMW 27616), Juxtlahuaca Cave, Guerrero, Mexico. **E**, **F**: *Paraphrynus carolynae* Armas, 2012, female (NHMW 27618), Tucson, Arizona, U.S.A. Scale bars: 0.5 mm.

Habitat. The type locality is a hill (1200–1300 m) covered by tropical dry forest dominated by bushes and low trees (Fig. 1E,F), e.g., *Brahea dulcis* (Kunth) Mart., *Ceiba aesculifolia* (Kunth) Britten & Baker, *Ficus* sp., cacti, e.g., *Opuntia depressa* Rose and *Pachycereus weberi* (J.M. Coult.) Backeb., which alternate with crop fields of *Areca* L. palms.

Whip spiders were collected from under stones and logs, mostly in the vicinity of an abandoned railway tunnel. *Acanthophrynus coronatus* (Butler, 1873), another species of whip spider in the family Phrynidae, was found in sympatry.

Distribution. Presently known only from the type locality Cerro de los Túneles, near Anenecuilco, in the municipality Ayala, Morelos, Mexico (Fig. 2).

Extended diagnosis. *Paraphrynus pseudomexicanus* can be morphologically distinguished from its closest relatives, *P. carolynae* and *P. mexicanus*, based on the following characters (Table 6). The carapace dorsal surface is densely covered with coarse tubercles and the frontal process obsolete in *P. pseudomexicanus*, whereas the carapace dorsal surface is sparsely covered with fine granules and the frontal process well developed in the other species. The tritosternum ventral surface is densely hirsute posteriorly in *P. pseudomexicanus* but sparsely hirsute posteriorly in the other species. The pedipalp femur bears 7 dorsal and 8 ventral spines, the tibia 9 dorsal and 6 ventral spines, and the basitarsus 4 dorsal and 3 ventral spines in *P. pseudomexicanus*, whereas the femur bears 6 dorsal and 6 ventral spines, the tibia 7–9 dorsal and 6–7 ventral spines, and the basitarsus 3–4 dorsal and
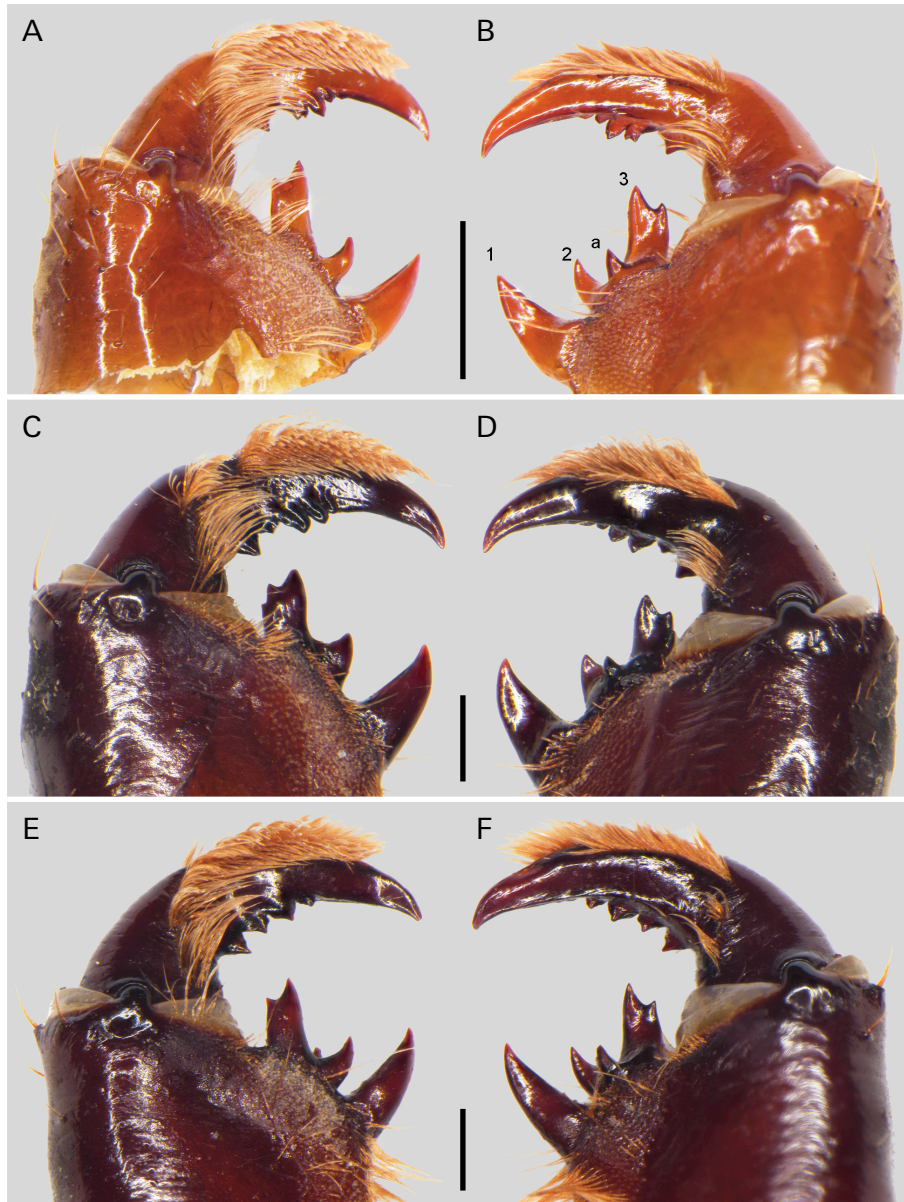
Fig. 4. *Paraphrynus* Moreno, 1940, cheliceral dentition, prolateral (**A**, **C**, **E**) and retrolateral (**B**, **D**, **F**) aspects (dense setae close to prolateral denticle row, at cheliceral base, removed). **A**, **B**: *Paraphrynus pseudomexicanus* sp.n., holotype female (NHMW 27612), Cerro de los Túneles, Morelos, Mexico. **C**, **D**: *Paraphrynus mexicanus* (Bilimek, 1867), male (NHMW 27615), Juxtlahuaca Cave, Guerrero, Mexico. **E**, **F**: *Paraphrynus carolynae* Armas, 2012, male (NHMW 27617), Tucson, Arizona, U.S.A. Scale bars: 1 mm (**A**, **B**), 0.5 mm (**C**–**F**).

3 ventral spines, in the other species. Leg I is comprised of 27 tibial and 59 tarsal articles in *P. pseudomexicanus* but 29 tibial articles and 60 tarsal articles in *P. carolynae*, and 27 tibial articles and 59 tarsal articles in *P. mexicanus*. Leg IV distitibia bears 22 trichobothria in *P. pseudomexicanus* but 24 and 21 trichobothria in *P. carolynae* and *P. mexicanus*, respectively. The female gonopod is evenly sclerotized with a broadened base extending into a rectilinear distal tip in *P. pseudomexicanus*, unlike the other species, in which the female gonopod is partly centric to evenly sclerotized with a slender to broadened base extending into a moderately to markedly curved distal tip. The male genitalia of *P. pseudomexicanus* bears a well-developed *processus internus* and the *lamina medialis* is obsolete whereas the *processus internus* is obsolete and the *lamina medialis* obsolete or well developed in the other species.

Paraphrynus pseudomexicanus can be morphologically distinguished from the other species of the *aztecus* group by the following characters: *P. pseudomexicanus* possesses 7 dorsal and VIII ventral spines on the pedipalp femur, whereas *P. aztecus*, *P. baeops*, *P. cubensis* and *P. pococki* each possess 6 dorsal and VI ventral spines; *P. pseudomexicanus* possesses 4 dorsal and III ventral spines on the pedipalp basitarsus, whereas *P. aztecus*, *P. baeops*, and *P. pococki* each possess 3 dorsal and III ventral spines, and *P. cubensis* possesses 3 dorsal and II ventral spines. In addition, the dorsal pedipalp tibial spines are long, the *lobus dorsalis* (male genitalia) well-developed and pointed, and the female gonopod sclerites rectilinear and basally broadened in *P. pseudomexicanus*, whereas the dorsal pedipalp tibial spines are noticeably shorter, the *lobus dorsalis* not visible dorsally, and the female gonopod sclerites rectilinear and evenly pointed in *P. cubensis*.

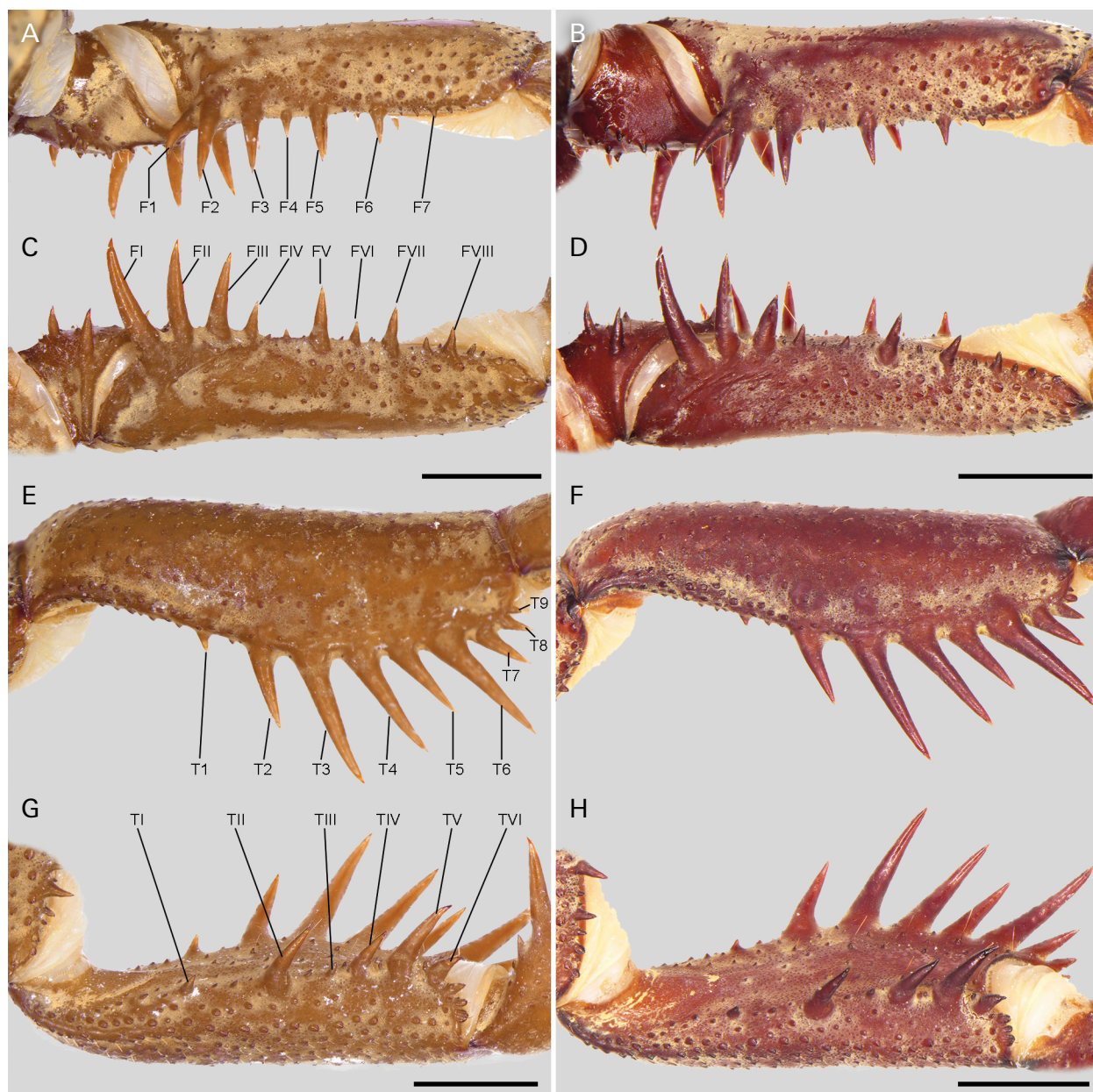**Etymology.** The new species name is a combination of the prefix *pseudo-*, meaning similar, and the word *mexi-*

Fig. 5. *Paraphrynus pseudomexicanus* sp.n., pedipalp trochanter and femur, dorsal (**A**, **B**) and ventral (**C**, **D**) aspects, and pedipalp tibia, dorsal (**E**, **F**) and prodorsal (**G**, **H**) aspects. **A**, **C**, **E**, **G**: Holotype female (NHMW 27612), Cerro de los Túneles, Morelos, Mexico. **B**, **D**, **F**, **H**: Paratype male (NHMW 28618), Cerro de los Túneles, Morelos, Mexico. Scale bars: 2 mm.

canus, referring to the morphologically most similar species, *P. mexicanus*.

Description of holotype female. *Color*: Carapace, opisthosoma and legs uniformly light grey to brown (Fig. 1A, B); carapace bordered by narrow white band; opisthosomal tergites with darker spots; pedipalps light reddish to dark brown depending on specimen age. ***Carapace*:** 1.39 times wider than long (Table 7). Dorsal surface densely covered with coarse tubercles, anterior margin with few fine tubercles. Frontal process obsolete, slightly visible in dorsal view. Ocelli well developed, elevated; lateral ocelli tri-ocular, median ocelli bi-ocular ellipsoid (Figs. 1A,B, 3A). ***Chelicerae*:** Surfaces granular, finely and densely setose, with many setaceous tubercles. Prolateral row of teeth

comprising three cuspid denticles (Fig. 4A,B); ventralmost tooth (distal: 3) largest; dorsalmost tooth (proximal: 1) bicuspid, upper cusp largest; retrolateral row with one tooth (a) cuspid (3 > 1 > 2 > a); claw (moveable finger) with five prominent teeth; proximal tooth largest, cuspid; second bicuspid (holotype only). ***Sternum*:** Cuticle soft, unsclerotized; three small, sclerotized sternites bearing setae. First sternite (tritosternum) elongated with paired subapical setae, tip of tritosternum broadly projecting between pedipalp coxae, bearing six setae posteriorly (Fig. 3B); second and third sternites small, oval to ellipsoid, each bearing two small setae. Pedipalp gnathocoxa (ventral surface) with broad surface of narrow, reddish setae on broad white mesal surface. ***Pedipalps*:** Surfaces coarsely tuberculate. Trochanter prodorsal surface with row
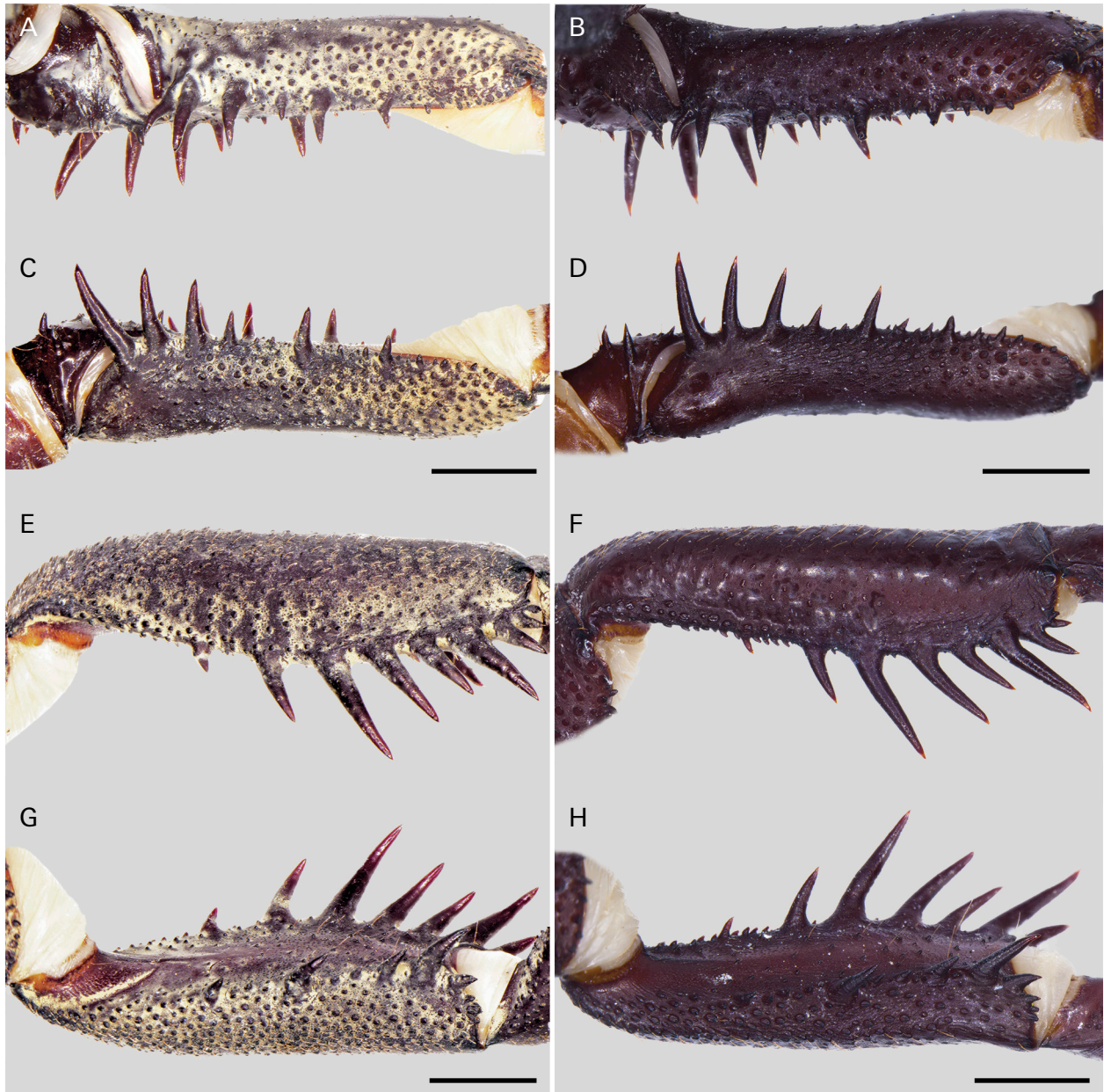
Fig. 6. *Paraphrynus* Moreno, 1940, pedipalp trochanter and femur, dorsal (**A**, **B**) and ventral (**C**, **D**) aspects, and pedipalp tibia, dorsal (**E**, **F**) and prodorsal (**G**, **H**) aspects. **A**, **C**, **E**, **G**: *Paraphrynus mexicanus* (Bilimek, 1867), male (NHMW 27615), Juxtlahuaca Cave, Guerrero, Mexico. **B**, **D**, **F**, **H**: *Paraphrynus carolynae* Armas, 2012, male (NHMW 27617), Tucson, Arizona, U.S.A. Scale bars: 2 mm.

of six small spines, proventral surface with two large spines and several smaller spinelets, interspersed with setaceous tubercles (Fig. 5A,C,E,G). Femur prodorsal margin with seven major spines (Fig. 5A,C,E,G), F2 largest, F1 and F2 sharing same base (F2 > F3 > F1 > F5 > F6 > F4 > F7); prolateral surface with many large, thickened tubercles; proventral margin with eight major spines, FI largest (FI > FII > FIII > FV > FVII > FIV > FVIII > FVI), interspersed with several small spines. Tibia with nine major dorsal spines, T3 largest (T3 > T6 > T4 > T5 > T2 > T7 > T8 > T1 > T9); proventral margin with six major spines, TV largest (TV > TII > TIV > TVI > TI > TIII), interspersed with one or more small spinelets. Basitarsus prodorsal margin with four large spines submedially (Fig. 7 A−C), sp2 (=lsmd-s) largest, one

small spine at base of sp3 and distal to sp4 (lsmd-s > sp4 > sp1 > sp3); proventral margin with three large spines, spII (=lsmv-s) largest, one small spine at base of spIII; distal margin with two long, apically thickened setae (rs) adjacent to spIII; prolateral surface with few well-developed spines proximally. Tarsus aspinose with well-developed cleaning organ, comprising short row of setae (coss) dorsally and long row of setae (co-ls) ventrally. Pretarsus (claw) not separated from tarsus (Fig. 7A−C). *Legs*: Dextral and sinistral antenniform legs comprising 38/27 tibial and 70/59 tarsal articles, respectively (Table 6), difference probably due to regeneration of dextral leg. Walking legs slightly elongated; leg IV basitibia trisegmented, third segment with single trichobothrium bt medially; distitibia with 22/22 trichobothria (Fig. 9A),
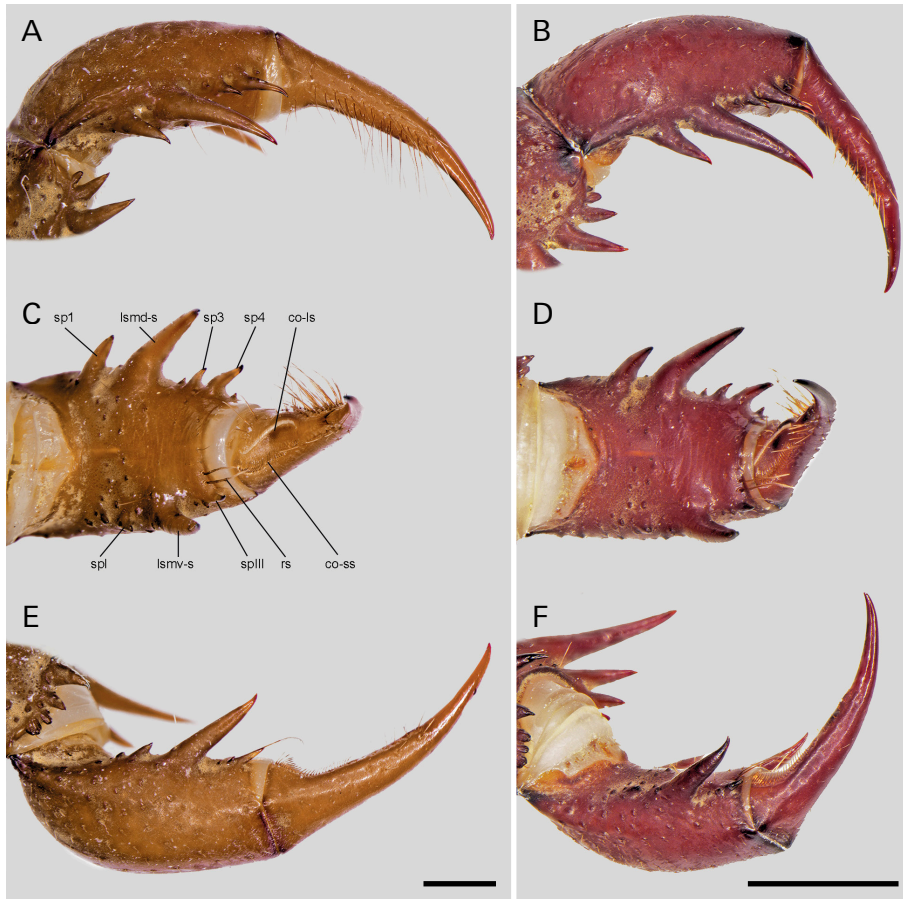
Fig. 7. *Paraphrynus pseudomexicanus* sp.n., pedipalp basitarsus and pretarsus, prodorsal (**A**, **B**), prolateral (**C**, **D**), and proventral (**E**, **F**) aspects. **A**, **C**, **E**: Holotype female (NHMW 27612), Cerro de los Túneles, Morelos, Mexico. **B**, **D**, **F**: Paratype male (NHMW 28618), Cerro de los Túneles, Morelos, Mexico. Scale bars: 1 mm (A, C, E), 2 mm (B, D, F).
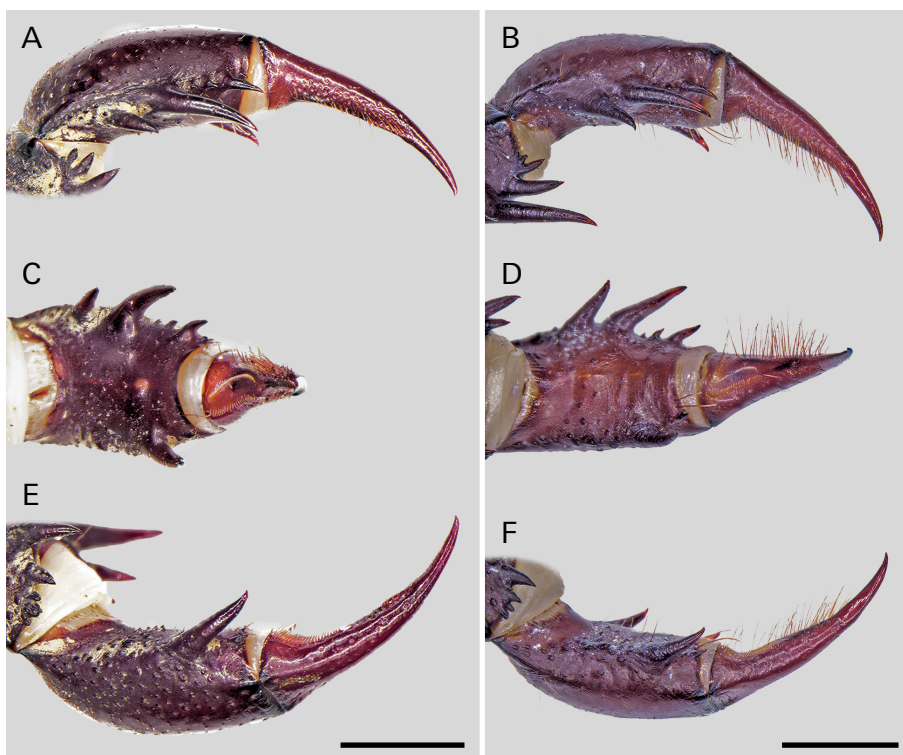

Fig. 8. *Paraphrynus* Moreno, 1940, pedipalp basitarsus and pretarsus, prodorsal (**A**, **B**), prolateral (**C**, **D**), and proventral (**E**, **F**) aspects. **A**, **C**, **E**: *Paraphrynus mexicanus* (Bilimek, 1867), male (NHMW 27615), Juxtlahuaca Cave, Guerrero, Mexico. **B**, **D**, **F**: *Paraphrynus carolynae* Armas, 2012, male (NHMW 27617), Tucson, Arizona, U.S.A. Scale bars: 2 mm.

sinistrally and dextrally (distances: distitibia total length 6.75; bt to bf 3.39, bf to sbf 0.64, sbf to bc 0.60, bc to stc1 2.08, stc1 to stf1 0.11); tarsi with slight transverse line, arolium absent in adult. **Gonopods:** Evenly sclerotized, with two claw-like appendages, hard and cuspid, basally broadened, rectilinear without curved tips (Fig. 10A,B).

Fig. 9. *Paraphrynus* Moreno, 1940, leg IV, basitibia and distitibia, prolateral aspect illustrating number and arrangement of basitibial and distitibial trichobothria. **A**: *Paraphrynus pseudomexicanus* sp.n., holotype female (NHMW 27612), Cerro de los Túneles, Morelos, Mexico. **B**: *Paraphrynus mexicanus* (Bilimek, 1867), male (NHMW 27615), Juxtlahuaca Cave, Guerrero, Mexico. **C**: *Paraphrynus carolynae* Armas, 2012, male (NHMW 27617), Tucson, Arizona, U.S.A. Scale bars: 2 mm (A, B), 1 mm (C).

Description of paratype male. *Habitus*: Resembles female holotype; lacking obvious secondary sexual dimorphism (Table 7, Figs. 5B,D,F,H, 7D – F). ***Male genitalia*:** Covered ventrally by genital operculum; operculum

Table 7. *Paraphrynus pseudomexicanus* sp.n.., measurements (mm) and meristic data for holotype and paratype deposited in the Naturhistorisches Museum, Wien, Austria (NHMW). Counts for legs I and IV refer to sinistral and dextral sides; other measurements are reported from one side only. Note: [1] count on dextral antenniform leg probably aberrant due to leg regeneration (see text for comments).

		Holotype ♀	Paratype ♂
		NHMW 27612	NHMW 28618
Carapace	Length	8.06	6.16
	Width	11.17	8.26
	Distance between lateral ocelli	3.63	2.57
Pedipalp	Femur	6.57	4.51
	Tibia	8.02	5.89
	Basitarsus	3.69	2.59
	Tarsus	3.64	2.44
Leg I	Tibial articles	27/38[1]	27/-
	Tarsal articles	59/70[1]	59/-
Leg II	Femur	12.87	9.20
Leg III	Femur	13.64	9.54
	Patella	2.15	1.345
	Basitibia	12.82	10.02
	Distitibia	7.07	5.57
	Basitarsus+claw	4.42	3.22
Leg IV	Femur	11.41	7.94
	Patella	1.82	1.49
	Basitibia	11.79	8.77
	Basitibia division	3/3	3/3
	Distitibia	6.26	5.04
	Distitibial trichobothria	22/22	22/22
	Basitarsus+claw	3.78	3.14

bearing several setae along anterior margin (Fig. 11A, B). LoL1 and LoL2 blunt, LoL2 one-third length of LoL1; PI large, blunt; LaM small, cuspid. ***Measurements*:** see Table 7.

3.3. Molecular systematics

The concatenated Q-INS-i alignments were slightly longer, with fewer parsimony-informative sites, than the G-INS-i and L-INS-i alignments (Table 4). The tree topologies recovered by analyses of the concatenated alignments with ML and BI, partitioned by gene, were mostly congruent, except for the positions of *P. aztecus* and *P. cubensis*, which varied among the analyses (Table 5). Most clades were consistently recovered with high bootstraps ($86\% \le x \le 100\%$) and moderate to high posterior probabilities ($0.76 \le x \le 1$) in the ML and BI trees, respectively, with the highest bootstraps for all clades recovered in the ML tree obtained by analysis of the Q-INS-i alignment (Fig. 12). The final optimization likelihood probabilities for the G-INS-i, Q-INS-i, and L-INS-i alignments were −12426.165885, −12234.231363 and −12409.810497, respectively. The ML and BI topologies closely resembled the topologies obtained by the parsimony analyses, differing only in the positions of *P. aztecus* and *P. cubensis* in all alignments, and in the position of *P. baeops* in the Q-INS-i alignment (Table 5).

Table 8. Uncorrected pairwise genetic distances of the mitochondrial COI locus for eight terminals representing all six described species in the *P. aztecus* group: *Paraphyrnus aztecus* (Pocock, 1894); *Paraphrynus baeops* (Mullinex, 1975); *Paraphrynus carolynae* Armas, 2012; *Paraphrynus cubensis* Quintero, 1983; *Paraphrynus mexicanus* (Bilimek, 1867); and *Paraphrynus pococki* Mullinex, 1975 and two samples of the new species, *Paraphyrnus pseudomexicanus* sp.n.

	2906	8667	14444	13883	15431	2091	14443
P. aztecus 2906							
P. baeops 8667	0.182						
P. carolynae 14444	0.184	0.190					
P. cubensis 13883	0.170	0.195	0.195				
P. mexicanus 15431	0.201	0.190	0.199	0.205			
P. pococki 2091	0.182	0.198	0.164	0.185	0.195		
P. pseudomexicanus 14443	0.195	0.196	0.202	0.185	0.160	0.211	
P. pseudomexicanus 14450	0.195	0.196	0.202	0.185	0.160	0.211	0.000
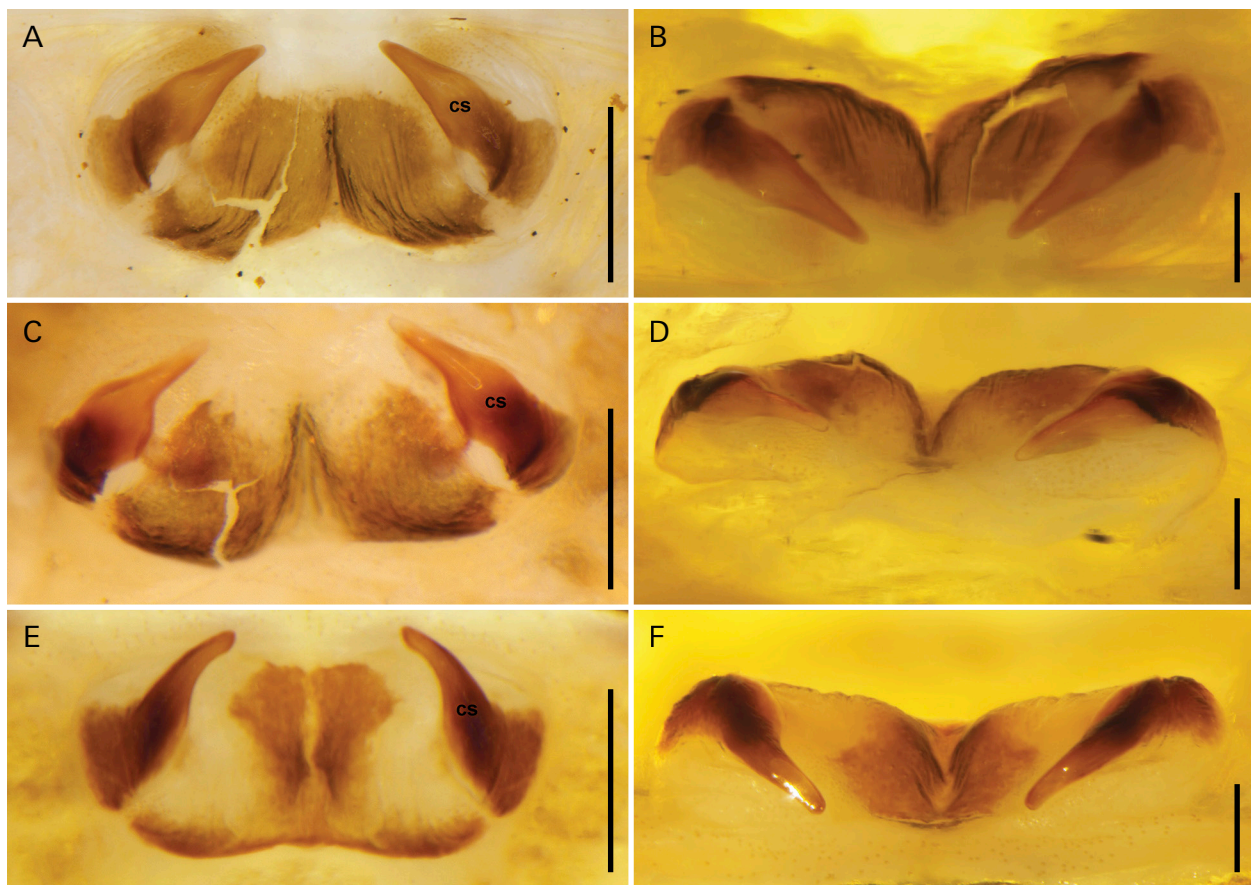
Fig. 10. *Paraphrynus* Moreno, 1940, female genitalia, dorsal (**A**, **C**, **E**) and posterior (**B**, **D**, **F**) aspects. **A**, **B**: *Paraphrynus pseudomexicanus* sp.n., holotype female (NHMW 27612), Cerro de los Túneles, Morelos, Mexico. **C**, **D**: *Paraphrynus mexicanus* (Bilimek, 1867), female (NHMW 27616), Juxtlahuaca Cave, Guerrero, Mexico. **E**, **F**: *Paraphrynus carolynae* Armas, 2012, female (NHMW 27618), Tucson, Arizona, U.S.A. Scale bars: 0.5 mm (A, C, E), 0.2 mm (B, D, F).

The COI sequences of the two samples of *P. pseudomexicanus* sp.n. were identical and differed most from *P. carolynae* and least from *P. mexicanus* (pairwise genetic distances, 20.2% and 16.0%; respectively Table 8).

3.4. Karyotypes

Three species of *Paraphrynus*, i.e., *P. aztecus*, *P. carolynae*, and *P. cubensis*, exhibited similar karyotypes, comprising a relatively low number of chromosomes ($2n\male = 30\text{–}36$) with exclusively biarmed (i.e., metacentric and submetacentric) morphology. The chromosome pairs decreased gradually in size (Fig. 13, Table S2). The chromosomes of *P. aztecus* ($2n\male = 36$) were metacentric except for four submetacentric pairs (Nos 3, 7, 14, 15) (Table S2). The karyotypes of *P. carolynae* ($2n\male = 30$) and *P. cubensis* ($2n\male = 34$) contained fewer submetacentric pairs, i.e., three pairs (Nos 1, 2, 12) and one pair (No. 12), respectively (Table S2). The chromosomes of *P. mexicanus* were also exclusively biarmed and decreased gradually in size (Fig. 13, Table S2). However, the diploid number of this species ($2n\male = 24$) was considerably lower than in the previously mentioned taxa
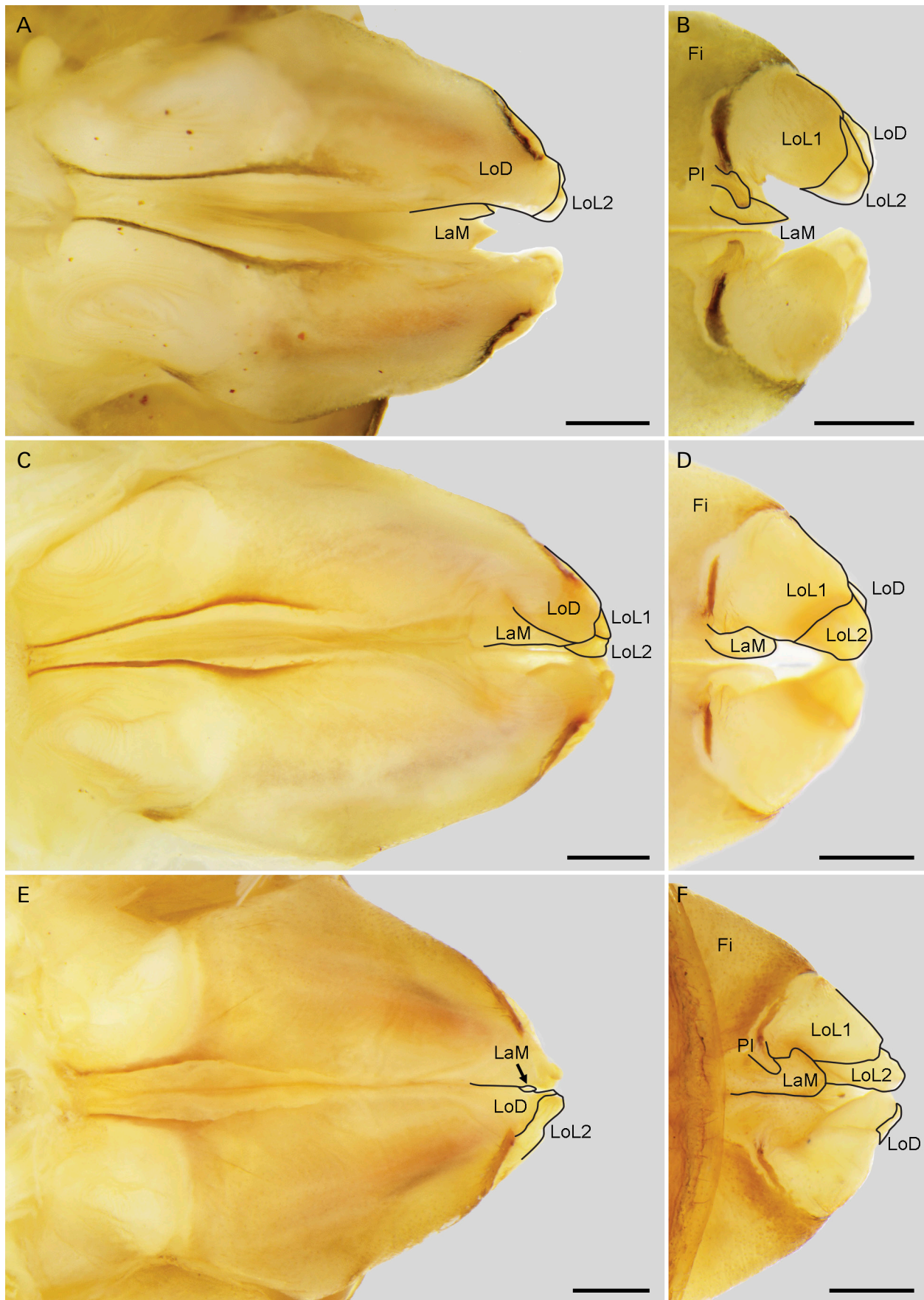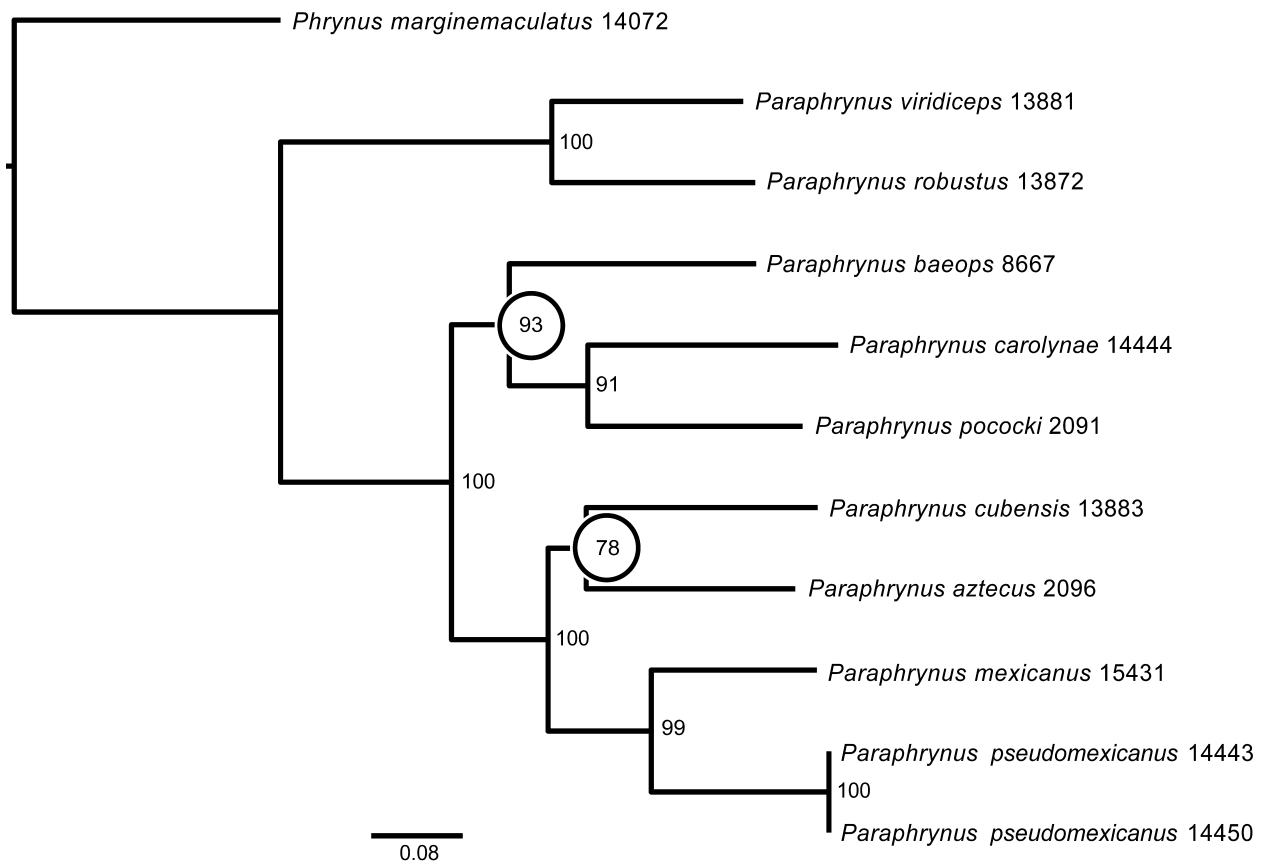
Fig. 11. *Paraphrynus* Moreno, 1940, spermatophore, dorsal (**A**, **C**, **E**) and ventral (**B**, **D**, **F**) aspects. **A**, **B**: *Paraphrynus pseudomexicanus* sp.n., paratype male (NHMW 28618), Cerro de los Túneles, Morelos, Mexico. **C**, **D**: *Paraphrynus mexicanus* (Bilimek, 1867), male (NHMW 27615), Juxtlahuaca Cave, Guerrero, Mexico. **E**, **F**: *Paraphrynus carolynae* Armas, 2012, male (NHMW 27617), Tucson, Arizona, U.S.A. Scale bars: 0.5 mm.

Fig. 12. Maximum Likelihood phylogeny of *Paraphrynus* Moreno, 1940 whip spiders, based on 3909 aligned nucleotides of DNA sequence from three mitochondrial and two nuclear gene loci (final optimization likelihood probabilities for Q-INS-i alignment of −12234.231363). Numbers following species refer to tissue samples (Table 2). Bootstrap support values indicated at nodes. Circles indicate two nodes that collapsed in the strict consensus of all analyses (Table 5).

(Fig. 12, Table S2). The new species ($2n\male = 32$) differed from the other species analyzed in containing mono-armed pairs. Eight pairs were metacentric (Nos 1, 2, 4, 6, 10, 11, 13, 16), one submetacentric (No. 14), and seven acrocentric (Nos 3, 5, 7−9, 12, 15) (Fig. 13, Table S2). The chromosome pairs of this species also decreased gradually in size (Fig. 13, Table S2).

The two other species investigated, *Paraphrynus robustus* and *Phrynus marginemaculatus*, each exhibited much higher diploid numbers. These species exhibited similar diploid numbers and proportions of particular chromosome types. Their karyotypes were dominated by biarmed chromosomes. In *P. robustus* ($2n\male = 64$), sixteen pairs were metacentric (Nos 1−3, 8, 10, 11, 13, 14, 16, 18, 20−24, 28), six submetacentric (Nos 4, 9, 26, 29, 31, 32), two subtelocentric (Nos 15, 30), and eight acrocentric (Nos 5−7, 12, 17, 19, 25, 27) (Fig. 13, Table S2). Chromosome pairs decreased discontinuously in size, forming two size groups: first to third pair (8.52−7.11% of TCL) and fourth to thirty-second pair (from 5.67 to 1.02% of TCL) (Table S2). The karyotype of *P. marginemaculatus* ($2n\male = 68$) comprised fourteen metacentric pairs (Nos 8, 13, 16, 17, 19−21, 24−26, 28−30, 34), five submetacentric pairs (Nos 1, 3, 10, 27, 31), five subtelocentric pairs (Nos 4, 9, 11, 12, 18), and ten acrocentric pairs (Nos 2, 5−7, 14, 15, 22, 23, 32, 33). The

chromosome pairs decreased gradually in size (Fig. 14, Table S2). Study of the karyotype did not reveal morphologically differentiated sex chromosomes in males of *Phrynus* and *Paraphrynus*.

4. Discussion

Mexico is a biodiversity hotspot for many animal taxa, including tarantulas, ricinuleids and scorpions (e.g. Mendoza & Francke 2017; Valdez-Mondragón et al. 2018; Quijano-Ravell et al. 2019), and whip spiders are no exception (e.g. Armas & Trujillo 2018; Armas et al. 2017). The country is inhabited by a diverse assemblage of whip spider species in three genera of the family Phrynidae. The greatest species diversity occurs in *Paraphrynus* (Harvey 2003, 2013), which has long been a source of taxonomic confusion (Mullinex 1975; Quintero 1983).

The present study focused on species of the *aztecus* group of *Paraphrynus*. Morphological data suggested the presence of an undescribed species, closely related to *P. mexicanus*, based on subtle character differences. Additional sources of evidence, specifically karyotype and

Fig. 13. Male karyotypes of *Paraphrynus* Moreno, 1940 whip spiders, based on plates formed by two sister metaphases II, Giemsa staining. **A**: *Paraphrynus aztecus* Pocock, 1894 (2n=36). **B**: *Paraphrynus carolynae* Armas, 2012 (2n=30). **C**: *Paraphrynus cubensis* Quintero, 1983 (2n=34). **D**: *Paraphrynus mexicanus* (Bilimek, 1867) (2n=24). **E**: *Paraphrynus pseudomexicanus* sp.n. (2n=32). **F**: *Paraphrynus robustus* (Franganillo, 1931) (2n=64). Scale bars: 10 μm (**A**, **C**, **D**, **E**), 5 μm (**B**, **F**).
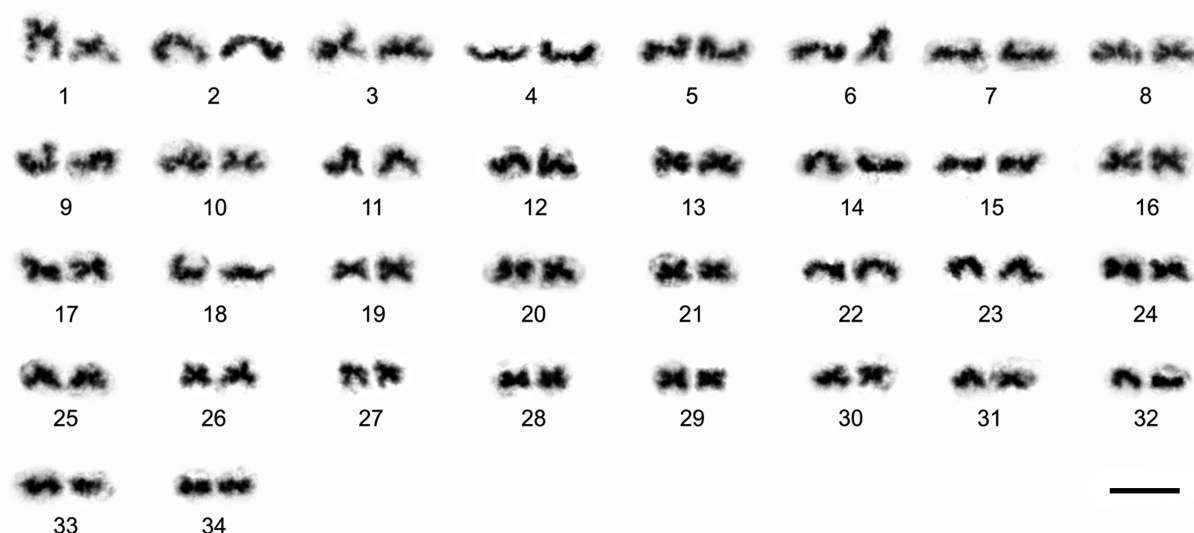
Fig. 14. Male karyotype of the whip spider, *Phrynus marginemaculatus* C.L. Koch, 1840 (2n = 68), based on plate formed by two sister metaphases II, Giemsa staining. Scale bar: 10 μm.
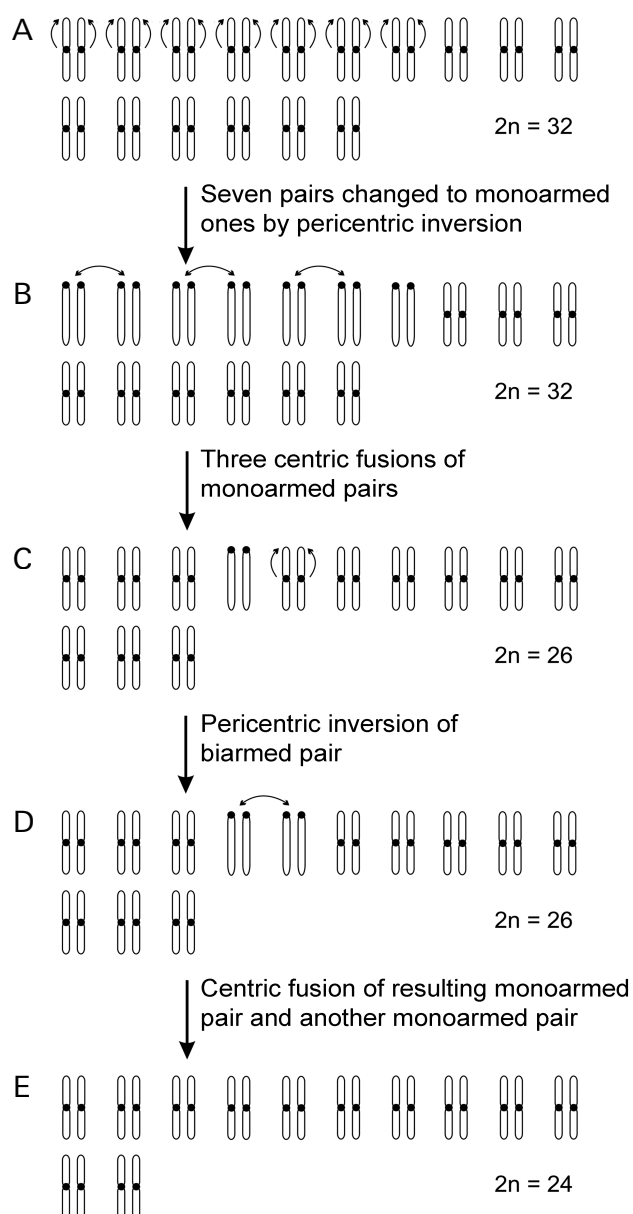
DNA sequence data, were sought to independently test the hypothesis of a new species. A phylogeny based on five loci from the nuclear and mitochondrial genomes, widely used in arachnid molecular systematics (SANTI-BÁNEZ-LÓPEZ et al. 2014; OJANGUREN AFFILASTRO et al. 2016; MENDOZA & FRANCKE 2017) consistently supported the hypothesis of a new species and its close relationship with *P. mexicanus*. Genetic divergence between the new species and its sister species was similar to divergence among other species examined. Additional support for the new species was provided by karyotype data, also in widespread use for several other arachnid orders (NOR-TON et al. 1993; KRÁL et al. 2008; ARAUJO et al. 2020; SCHNEIDER et al. 2020; ŠŤÁHLAVSKÝ et al. 2020; TSURUSAKI et al. 2020) and known to exhibit a high level of diversity in whip spiders (J. Král, unpublished data 2020). Karyotype data suggested the new species and its sister taxon, *P. mexicanus*, are separated by several chromosome rearrangements (probably centric fusions and inversions). These rearrangements are usually involved in the formation of interspecific barriers and speciation (e.g., RIESEN-BERG 2001; NOOR et al. 2001; KIRKPATRICK & BAXTON 2006; LOWRY & WILLIS 2010; FEDER et al. 2014). As with another phrynid, *Heterophrynus* Pocock, 1894 (PAULA-NETO et al. 2013), the males of *Paraphrynus* and *Phrynus* did not exhibit morphologically differentiated sex chro-

---

← **Fig. 15.** Hypothesis of karyotype evolution in a clade of whip spiders comprising *Paraphrynus mexicanus* (Bilimek, 1867) and *Paraphrynus pseudomexicanus* sp.n. **A**: Hypothesized common ancestral karyotype of *P. mexicanus* and *P. pseudomexicanus* (2n = 32, biarmed chromosomes). **B**: Karyotype of *P. pseudomexicanus* (2n = 32, biarmed chromosomes except for seven acrocentric pairs). **C**, **D**: Hypothesized intermediates between karyotypes of *P. pseudomexicanus* and *P. mexicanus* (**C**: 2n = 26, biarmed chromosomes except for one acrocentric pair, **D**: 2n = 26, biarmed chromosomes except for two acrocentric pairs). **E**: Karyotype of *P. mexicanus* (2n = 24, biarmed chromosomes).

mosomes. No data on sex chromosomes are available from the other whip spiders.

Comparison of genomic and chromosome data also permitted a reconstruction of karyotype evolution in *Paraphrynus* in light of the molecular phylogeny. The data indicate the ancestral diploid number of the clade formed by *Phrynus* and *Paraphrynus* comprised approximately 70 chromosomes, close to the hypothesized original diploid number for Phrynoidea (J. Král, unpublished data 2020). Karyotype similarity between *Phrynus marginemaculatus* and *Paraphrynus robustus* might reflect a relatively basal position of the latter species in the *Paraphrynus* tree. The karyotype of *P. robustus* differs from the chromosome complement of *P. marginemaculatus* in possessing a slightly lower diploid number and higher portion of biarmed chromosome pairs. This pattern suggests the number of biarmed pairs in *P. robustus* increased mostly by centric fusions of monoarmed (subtelocentric and acrocentric) pairs. Subsequent evolution in *Paraphrynus* was apparently accompanied by a considerable decrease in the diploid number, which involved centric fusions of remaining monoarmed pairs. This process resulted in a karyotype saturated by biarmed chromosomes. Based on the results presented here, the ancestral karyotype of the *aztecus* group probably comprised 30–36 biarmed chromosomes. The common ancestor of *P. mexicanus* and the new species probably exhibited 32 biarmed chromosomes (Fig. 15). The karyotype of the new species subsequently evolved from this pattern by pericentric inversions of seven biarmed pairs, changing the morphology of these pairs to acrocentric. The evolution of *P. mexicanus* included fusions of acrocentric pairs observed in the new species (Fig. 15).

In conclusion, data from morphology, karyotype and DNA illuminated the understanding of diversity and phylogeny in members of the genus *Paraphrynus*, independently supporting the recognition of a new species described above, and illustrating the utility of an integrative approach to the systematics of whip spiders.

5.   Acknowledgements

7.   References

Araujo D., Schneider M.C., Paula-Neto E., Cella D.M. 2020. The spider cytogenetic database. – URL <http://www.arthropodacytogenetics.bio.br/spiderdatabase> [accessed 29 February 2020].

Armas L.F. 2012. A new species of *Paraphrynus* Moreno, 1940 (Amblypygi: Phrynidae) from Mexico and the south-west of the United States. – Revista Ibérica de Aracnología **21**: 27–32.

Armas L.F., Trujillo R.E. 2018. Una especie nueva del género *Paraphrynus* de Chiapas, México (Amblypygi: Phrynidae). – Revista Ibérica de Aracnología **32**: 81–85.

Armas L.F., Quijano-Ravell A.F., Ponce-Saavedra J. 2017. A new species of *Phrynus* from western Mexico and new localities for some whip spiders from Michoacán and Guerrero (Amblypygi: Phrynidae). – Revista Ibérica de Aracnología **30**: 47–52.

Ballesteros J.A.C. 2010. Sistemática filogenética del género *Paraphrynus* Moreno (Arachnida: Amblypygi: Phrynidae). – Tesis Digitales, Universidad Nacional Autónoma de México, Mexico City.

Chapin K.J. 2014a. Cave-epigean behavioral variation of the whip spider *Phrynus longipes* (Arachnida: Amblypygi) evidenced by activity, vigilance, and aggression. – Journal of Arachnology **43**: 214–219.

Chapin K.J. 2014b. Microhabitat and spatial complexity predict group size of the whip spider *Heterophrynus batesii* in Amazonian Ecuador. – Journal of Tropical Ecology **30**: 173–177.

Chapin K.J., Reed-Guy S. 2017. Territoriality mediates atypical size-symmetric cannibalism in the Amblypygi *Phrynus longipes*. – Ethology **123**: 1–6.

Darriba D., Taboada G.L., Doallo R., Posada D. 2012. jModelTest 2: More models, new heuristics and parallel computing. – Nature Methods **9**: 772–774.

Dayrat B. 2005. Towards integrative taxonomy. – Biological Journal of the Linnean Society **85**: 407–415.

Dolejš P., Kořínková T., Musilová J., Opatová V., Kubcová L., Buchar J., Král J. 2011. Karyotypes of central European spiders of the genera *Arctosa, Tricca*, and *Xerolycosa* (Araneae: Lycosidae). – European Journal of Entomology **108**: 1–16.

Dunlop J.A. 1994. An Upper Carboniferous amblypygid from the Writhlington Geological Nature Reserve. – Proceedings of the Geologists' Association **105**: 245–250.

Feder J.L., Nosil P., Flaxman S.M. 2014. Assessing when chromosomal rearrangements affect the dynamics of speciation: Implications from computer simulations. – Frontiers in Genetics **5**: 295.

Filippov A.È., Wolff J.O., Seiter M., Gorb S. 2017. Numerical simulation of colloidal self-assembly of super-hydrophobic arachnid cerotegument structures. – Journal of Theoretical Biology **430**: 1–8.

Folmer O., Black M.B., Hoch W., Lutz R.A., Vrijenhoek R.C. 1994. DNA primers for amplification of mitochondrial Cytochrome *c* Oxidase subunit I from diverse metazoan invertebrates. – Molecular Marine Biology and Biotechnology **3**: 294–299.

Giupponi A.P., Kury A. 2013. Two new species of *Heterophrynus* Pocock, 1894 from Colombia with distribution notes and a new synonymy (Arachnida: Amblypygi: Phrynidae). – Zootaxa **3647**: 329–342.

Goloboff P.A. 1993. Estimating character weights during tree search. – Cladistics **9**: 83–91.

Goloboff P.A., Farris J.S., Nixon K.C. 2003. TNT: Tree Analysis Using New Technology. Computer software and documentation. – URL <http://www.zmuc.dk/public/Phylogeny/TNT> [accessed 29 February 2020]

Goloboff P.A., Farris J.S., Nixon K.C. 2008. TNT, a free program for phylogenetic analysis. – Cladistics **24**: 774–786.

Guindon S., Gascuel O. 2003. A simple, fast and accurate method to estimate large phylogenies by maximum-likelihood. – Systematic Biology **52**: 696–704.

HARVEY M.S. 2003. Catalogue of the smaller arachnid orders of the world: Amblypygi, Uropygi, Schizomida, Palpigradi, Ricinulei and Solifugae. – CSIRO Publishing, Collingwood, Australia.

HARVEY M.S. 2013. Whip spiders of the world, version 1.0., Perth: Western Australian Museum. – URL <http://museum.wa.gov.au/catalogues-beta/whip-spiders> [accessed 29 February 2020]

HEBETS E.A., ACEVES-APARICIO A., AGUILAR-ARGÜELLO S., BINGMAN V.P., ESCALANTE I., GERING E.J., NELSEN D.R., RIVERA J., SÁNCHEZ-RUIZ J.A., SEGURA-HERNÁNDEZ L., SETTEPANI V., WEIGMANN D.D., STAFSTROM J.A. 2014a. Multimodal sensory reliance in the nocturnal homing of the amblypygid *Phrynus pseudoparvulus* (Class Arachnida, Order Amblypygi). – Behavioural Processes **108**: 123–130.

HEBETS E.A., GERING E.J., BINGMAN V.P., WIEGMANN D.D. 2014b. Nocturnal homing in the tropical amblypygid *Phrynus pseudoparvulus* (Class Arachnida, Order Amblypygi). – Animal Cognition **17**: 1013–1018.

KATOH K., KUMA K., TOH H., MIYATA T. 2005. MAFFT version 5: Improvement in accuracy of multiple sequence alignment. – Nucleic Acids Research **33**: 511–518.

KATOH M., KUMA M. 2002. MAFFT: A novel method for rapid multiple sequence alignment based on fast Fourier transform. – Nucleic Acids Research **30**: 3059–3066.

KIRKPATRICK M., BARTON N. 2006. Chromosome inversions, local adaptation and speciation. – Genetics **173**: 419–434.

KOCHER T.D., THOMAS W.K., MEYER A., EDWARDS S.V., PÄÄBO S., VILLABLANCA F.X., WILSON A.C. 1989. Dynamics of mitochondrial DNA evolution in animals: Amplification and sequencing with conserved primers. – Proceedings of the National Academy of Sciences, U.S.A. **86**: 6196–6200.

KRÁL J., KOVÁČ Ľ., ŠŤÁHLAVSKÝ F., LONSKÝ P., ĽUPTÁČIK P. 2008. The first karyotype study in palpigrades, a primitive order of arachnids (Arachnida: Palpigradi). – Genetica **134**: 79–87.

KUMAR S., STECHER G., LI M., KNYAZ C., TAMURA K. 2018. MEGA X: Molecular Evolutionary Genetic Analysis across computing platforms. – Molecular Biology and Evolution **35**: 1547–1549.

LEVAN A.K., FREDGA K., SANDBERG A.A. 1964. Nomenclature for centromeric position on chromosomes. – Hereditas **52**: 201–220.

LOWRY D.B., WILLIS J.H. 2010. A widespread chromosomal inversion polymorphism contributes to a major life-history transition, local adaptation, and reproductive isolation. – PLoS Biology **8**: e1000500.

MENDOZA J.J., FRANCKE O.F. 2017. Systematic revision of *Brachypelma* red-kneed tarantulas (Araneae: Theraphosidae), and the use of DNA barcodes to assist in the identification and conservation of CITES-listed species. – Invertebrate Systematics **31**: 157–179.

MIRANDA DE G.S., GIUPPONI A.P.L., PRENDINI L., SCHARFF N. 2018. *Weygoldtia*, a new genus of Charinidae Quintero, 1986 (Arachnida, Amblypygi) with a reappraisal of the genera in the family. – Zoologischer Anzeiger **273**: 23–32.

MULLINEX C.L. 1975. Revision of *Paraphrynus* Moreno (Amblypygida: Phrynidae) for North America and the Antilles. – Occasional Papers of the California Academy of Sciences **116**: 1–80.

NOOR M.A.F., GRAMS K.L., BERTUCCI L.A., REILAND J. 2001. Chromosomal inversions and the reproductive isolation of species. – Proceedings of the National Academy of Sciences, U.S.A. **98**: 12084–12088.

NORTON R.A., KETHLEY J.B., JOHNSTON D.E., O'CONNOR B.M. Phylogenetic perspectives on genetic systems and reproductive modes of mites. Pp. 8–99 in WRENSCH D., EBBERT, M.A. (eds), Evolution and Diversity of Sex Ratio in Insects and Mites. – Chapman & Hall, New York, U.S.A.

NUNN G.B., THEISEN B.F., CHRISTENSEN B., ARCTANDER P. 1996. Simplicity-correlated size growth of the nuclear 28S ribosomal RNA D3 expansion segment in the crustacean order Isopoda. – Journal of Molecular Evolution **42**: 211–223.

OJANGUREN AFFILASTRO A.A., MATTONI C.I., OCHOA J.A., RAMÍREZ M.J., CECCARELLI F.S., PRENDINI L. 2016. Phylogeny, species delimitation and convergence in the South American bothriurid scorpion genus *Brachistosternus* Pocock 1893: Integrating morphology, nuclear and mitochondrial DNA. – Molecular Phylogenetics and Evolution **94**: 159–170.

PAULA-NETO E., ARAUJO D., CARVALHO L.S., CELLA D.M., SCHNEIDER M.C. 2013. Chromosomal characteristics of a Brazilian whip spider (Amblypygi) and evolutionary relationships with other arachnid orders. – Genetics and Molecular Research **12**: 3726–3734.

PRENDINI L. 2000. Phylogeny and classification of the Superfamily Scorpionoidea Latreille 1802 (Chelicerata, Scorpiones): An exemplar approach. – Cladistics **16**: 1–78.

PRENDINI L., WEYGOLDT P., WHEELER W.C. 2005. Systematics of the *Damon variegatus* group of African whip spiders (Chelicerata: Amblypygi): Evidence from behaviour, morphology and DNA. – Organisms, Diversity and Evolution **5**: 203–236.

QUIJANO-RAVELL A.F., ARMAS L.F., FRANCKE O.F., PONCE-SAAVEDRA J. 2019. A new species of the genus *Centruroides* Marx (Scorpiones, Buthidae) from western Michoacán State, México using molecular and morphological evidence. – ZooKeys **859**: 31–48.

QUINTERO D.J. 1981. The amblypygid genus *Phrynus* in the Americas (Amblypygi, Phrynidae). – Journal of Arachnology **9**: 117–166.

QUINTERO D.J. 1983. Revision of the amblypygid spiders of Cuba and their relationships with the Caribbean and continental American amblypygid fauna. – Studies on the Fauna of Curaçao and other Caribbean Islands **65**: 1–54.

RIESENBERG L.H. 2001. Chromosomal rearrangements and speciation. – Trends in Ecology and Evolution **16**: 351–358.

RONQUIST F., HUELSENBECK J.P. 2003. MrBayes 3: Bayesian phylogenetic inference under mixed models. – Bioinformatics **19**: 1572–1574.

SANTIBÁÑEZ-LÓPEZ C.E., FRANCKE O.F., PRENDINI L. 2014. Phylogeny of the North American scorpion genus *Diplocentrus* Peters, 1861 (Scorpiones: Diplocentridae) based on morphology, nuclear and mitochondrial DNA. – Arthropod Systematics and Phylogeny **72**: 257–279.

SCHNEIDER M.C., MATTOS V.F., CELLA D.M. 2020. The scorpion cytogenetic database. – URL <http://www.arthropodacytogenetics.bio.br/scorpiondatabase> [accessed 29 February 2020].

SEITER M., WOLFF J.O. 2017. *Stygophrynus orientalis* sp.n. (Amblypygi: Charontidae) from Indonesia with the description of a remarkable spermatophore. – Zootaxa **4232**: 397–408.

SEITER M., LANNER J. 2017. Description and first record of *Phrynus tessellatus* (Pocock, 1894) (Arachnida: Amblypygi: Phrynidae) from northwestern Trinidad, with the description of its mating behaviour. – Arachnology **17**: 201–209.

SEITER M., LANNER L., KAROLYI F. 2017. Mating behaviour and spermatophore morphology of four Cuban whip spiders (Arachnida, Amblypygi, Phrynidae). – Taxonomic relevance and evolutionary trends. – Zoologischer Anzeiger **269**: 117–126.

SIMON C., FRATI F., BECKENBACH A., CRESPI B., LIU H., FLOOK P. 1994. Evolution, weighting, and phylogenetic utility of mitochondrial gene sequences and a compilation of conserved polymerase chain reaction primers. – Annals of the Entomological Society of America **87**: 651–701.

ŠŤÁHLAVSKÝ F. 2020. The pseudoscorpion cytogenetic database. – URL <http://www.arthropodacytogenetics.bio.br/pseudoscorpiondatabase> [accessed 29 February 2020].

STAMATAKIS A. 2006. RAxML-VI-HPC: Maximum likelihood-based phylogenetic analyses with thousands of taxa and mixed models. – Bioinformatics **22**: 2688–2690.

STAMATAKIS A. 2014. RAxML version 8: A tool for phylogenetic analysis and post-analysis of large phylogenies. – Bioinformatics **30**: 1312–1313.

STECHER G., TAMURA K., KUMAR S. 2020. Molecular Evolutionary Genetics Analysis (MEGA) for macOS. – Molecular Biology and Evolution. https://doi.org/10.1093/molbev/msz312.

TSURUSAKI N., SVOJANOVSKÁ H., SCHÖENHOFER A., ŠŤÁHLAVSKÝ F. 2020. The harvestmen cytogenetic database. – URL <www.arthropodacytogenetics.bio.br/harvestmendatabase/index.html> [accessed 29 February 2020].

Valdez-Mondragón A., Francke O., Botero-Trujillo R. 2018. New morphological data for the order Ricinulei with the description of two new species of *Pseudocellus* (Arachnida: Ricinulei: Ricinoididae) from Mexico. – Journal of Arachnology **46**: 114 – 132.

Weygoldt P. 2000. Whip spiders. Their biology, morphology and systematics. – Apollo Books, Stenstrup, Denmark, 163 pp.

Wheeler W.C., Cartwright P., Hayashi C. 1993. Arthropod phylogeny: A combined approach. – Cladistics **9**: 1 – 39.

Wolff J.O., Schwaha T., Seiter M., Gorb S.N. 2016. Whip spiders (Amblypygi) become water-repellent by a colloidal secretion that self-assembles into hierarchical microstructures. – Zoological Letters **2**. https://doi.org/10.1186/s40851-016-0059-y

Wolff J.O., Seiter M., Gorb S.N. 2017. The water-repellent cerotegument of whip-spiders (Arachnida: Amblypygi). – Arthropod Structure and Development **46**: 116 – 129.

Yang Z. 1994. Maximum likelihood phylogenetic estimation from DNA sequences with variable rates over sites: Approximate methods. – Journal of Molecular Evolution **39**: 306 – 314.

Authors' contributions

Vargas organized the collecting permits and preparation of chromosome slides, and assisted during the field trip. Seiter coordinated the study and conducted the morphological analysis; Colmenares and Prendini generated the DNA sequence data; Loria conducted the DNA sequence analysis; Loria and Prendini wrote the sections on molecular systematics; Lerma, Král, Sember and Divišová generated the karyotype data and performed the analysis; Seiter, Král and Prendini wrote the manuscript; other authors revised the manuscript.

Conflicts of Interest

The authors declare no conflicts of interest.

Electronic Supplement Files

Electronic Supplement S1. Material used for analysis of cryptic diversity and phylogeny of whip spiders in the genus *Paraphrynus* Moreno, 1940, deposited in the Naturhistorisches Museum, Wien, Austria (NHMW); the Department of Genetics and Microbiology, Charles University, Prague, Czech Republic (JK); and the Ambrose Monell Cryocollection (AMCC) and the Collections of Arachnida and Myriapoda at the American Museum of Natural History (AMNH), New York, U.S.A.

Electronic Supplement S2. Chromosome data for species of the whip spider genera *Paraphrynus* Moreno, 1940 and *Phrynus* Lamarck, 1801 analysed karyologically. Abbreviations: A = acrocentric; CI = centromeric index; CM = chromosome morphology; M = metacentric; N = number of plates used to evaluate chromosome data; SD-CI = standard deviation of centromeric index; SD-RCL = standard deviation of relative chromosome length; SM = submetacentric; ST = subtelocentric; RCL = relative chromosome length.